JAERI 1218

JAERI 1218

# Evaluation of the Total Neutron Cross Section of Carbon up to 2 MeV

October 1971

日本原子力研究所

Japan Atomic Energy Research Institute

日本原子力研究所は，研究成果，調査結果などを JAERI レポートとして，つぎの４種に分けそれぞれの通し番号を付し，不定期に刊行しております．

| | | |
|---|---|---|
| 1. 研究報告 | まとまった研究の成果あるいはその一部における重要な結果の報告 | JAERI 1001- |
| 2. 調査報告 | 総説・展望・調査の結果などをまとめたもの | JAERI 4001- |
| 3. 年　　報 | 研究・開発その他の活動状況などの報告 | JAERI 5001- |
| 4. 資　　料 | 施設の概要や手引きなど | JAERI 6001- |

このうち既刊分については「JAERI レポート一覧」にタイトル・要旨をまとめて掲載し，また新刊レポートは「研究成果要旨集」(隔月刊)で逐次紹介しています．

これらのリスト・研究報告書の入手および複写・翻訳などのご要求は日本原子力研究所技術情報部（茨城県那珂郡東海村）に申しこんでください．

---

Japan Atomic Energy Research Institute publishes the nonperiodical reports with the following classification numbers:

1. JAERI 1001-　Research reports
2. JAERI 4001-　Survey reports and reviews
3. JAERI 5001-　Annual reports
4. JAERI 6001-　Manuals etc.

Requests for the above publications, and reproduction and translation should be addressed to Division of Technical Information, Japan Atomic Energy Research Insitute, Tokai-mura, Naka-gun, Ibaraki-ken, Japan

---

編集兼発行　日本原子力研究所
印　　刷　いばらき印刷

# Evaluation of the Total Neutron Cross Section of Carbon up to 2 MeV

Kazuaki NISHIMURA, Sin-iti IGARASI, Toyojiro FUKETA
and Shigeya TANAKA

Tokai Research Establishment,
Japan Atomic Energy Research Institute

Received May 21, 1971

## Abstract

Total neutron cross section of carbon has been evaluated in the energy range from 1 eV to 2 MeV. Fourth order polynomials of neutron energy are fitted to the collected experimental data by the method of least-squares. The assessment of the weight includes an account for the experimental errors of the individual data points, number of data points in the individual experiment and a weight given to the measurement by the present authors. The difference between the experimental cross-section data obtained by time-of-flight method and those by direct-current-beam method, and non-uniformity of distribution of the data points over the neutron energy range are discussed. A recommended value of the total neutron cross section of carbon is given as

$$\sigma_{nT}(E) = 4.699 - 3.061E + 1.069E^2 - 0.095E^3 - 0.026E^4,$$

where E is in MeV and $\sigma_{nT}$ in barns. Uncertainty of the recommended value is estimated to be less than 2 to 3% in the energy region up to 1.8 MeV. The cross-section curve is compared with those of BNL 325, ENDF/B, KFK 750 and AWRE data files.

# 2 MeVまでの炭素の中性子全断面積の評価

日本原子力研究所東海研究所

西村和明・五十嵐信一・更田豊治郎・田中茂也

1971年5月21日受理

## 要　　旨

1 eVから2 MeVまでの炭素の中性子全断面積が評価された。収集された実験データは，最小自乗法によりエネルギの4次式で適合された。最小自乗法における重みの査定には，個々の実験におけるデータ点の誤差，実験に含まれるデータ点の数，および現在の著者らによって個々の測定に与えられた重み，が考慮されている。飛行時間法と直流ビーム法により得られた実験データの間での差異，およびデータの分布の非一様性について議論されている。炭素の中性子全断面積の推奨される値が与えられている：

$$\sigma_{nT}(E) = 4.699 - 3.061\,E + 1.069\,E^2 - 0.095\,E^3 - 0.026\,E^4,$$

ここでEはMeV，$\sigma_{nT}$はbarns．推奨される値の不確定さは，1.8MeVまでの領域で2～3%以下と見積られる。断面積曲線は，BNL325，ENDF/B，KFK750およびAWRE データファイルの曲線と比較されている。

CONTENTS

# 目　　次

## 1. Introduction

The usefulness of the total neutron cross section of carbon as one of the standards for neutron flux measurements has been discussed[1] since 1965 at a subcommittee and panels of EANDC (European American Nuclear Data Committee) and INDC (International Nuclear Data Committee). The main reasons for the usefulness are the following:

(1) the major mode of the neutron reaction is elastic scattering in the energy region of interest, from 1 eV to 2 MeV. The only process competing with the scattering is the absorption, of which cross section is far smaller than thermal value of 3.4 mb[2]. (2) The angular distribution of scattered neutrons is reported as isotropic in the energy region less than about 50 keV[3], or 150 keV[4], and is almost isotropic below 1.0 MeV[5]. (3) The total cross section shows a monotonic shape with no resonance structure below 2.0 MeV. (4) Procurement of high purity carbon sample is easy in the form of solid.

During the last quarter century, many measurements on the total neutron cross section of carbon have been made in the energy regions up to 2 MeV. However, the experimental data show large discrepancy, say about 5 percent at 1 MeV, which is a serious problem for the use of the carbon cross section as a standard. Some experimenters deduced empirical formulae for the cross section based on their own experimental data[6-10]. The cross-section values of their formulae deviate from each other, and the energy regions to be applied to their cross-section formulae are limited within specific regions.

In such a circumstance, a refined evaluation work is highly necessary. Many evaluation papers on carbon cross section have been reported[4),11-13]. In most cases, however, the evaluation works were done in such a way that evaluators chose only some specified data sets which were considered to be more reliable among the various measurements and deduced a cross-section curve from those data sets according to their own procedures. Some other evaluators deduced their cross-section curve by using a number of data sets

which were available at that time, but it has passed more than several years after the publication of these papers.

With the recent advance of technical improvements, a large number of data points have been measured mainly by the time-of-flight method, and most of them are not included in the previous evaluation papers. It must be worthwhile to present a standard cross-section curve of high reliability by including all the data sets available at present with an assignment of a proper weight to each data set by critical judgement for the individual experiment.

In the present report, the least-squares method is applied to experimental data to derive empirical formulae, which are given by fourth order polynomials of neutron energy. In the earlier stage of this evaluation work, experimental data used as input to the computer were obtained mainly from SCISRS. At the later stage of this work, a large number of data points were obtained from NEUDADA, and were added to already acquired data. Then, the data sets used at the earlier and later stages are refered to as Data Set No. 1 and Data Set No. 2, respectively. Both data sets include many kinds of experimental data which have been taken under various conditions. These conditions are measures of critical judgement for the individual experimental data. In the next section, the characteristic items of inividdual data sets are given in tabular form associated with short notes. Status of original data is also presented in section 2.

In order to decide the method of evaluation, some critical considerations on the weight in the least-squares fit are discussed in section 3, where the experimental error of the individual data points, number of data points in one set, distribution of the data points over the neutron energy, and an evaluator's weight factor to individual experiment are taken into account.

Actual procedure of the least-squares fit with a rejection of the data and an assignment of weights is presented in section 4. The assignment of

weights to the experimental data points has been examined in detail by taking the following steps:

(1) First, weights to the individual data points were taken to be equal to each other. This step was applied to Data Set No. 1 at the earlier stage of this work.

(2) Second, the weight was taken to be proportional to inverse square of experimental error of each data point in Data Set No. 1 and No. 2.

(3) Finally, the weight was assigned in Data Set No. 2 by taking into account quality assessment to each experiment, number of data points in each data sets, and experimental error of each data points.

The results of these steps are presented in section 4. Although the results of the first step was reported elsewhere[14], the present paper is inclusive of the essential part of the previous report. Criteria for quality assessment in the final step are also described in section 4.

Discussions about the results of the calculations are given in section 5. Comparisons are made among the cross-section curves obtained with various kinds of weight and those obtained with different kinds of experimental methods. The present evaluated curves are compared with those evaluated by other investigators. Finally, a recommended value of the carbon total cross section is proposed with an assessment of error for the practical use.

The present study was initiated by a suggestion made by Dr. R. F. Taschek, LASL, U.S.A. and Dr. J. Spaepen, BCMN, Belgium at the 4th meeting of the INDSWG held at Tokyo, 1965, and has been performed as one of the programs of the Japanese Nuclear Data Committee.

## 2. Status of original data

### 1) Data compilation

The numerical data of carbon total neutron cross section have been collected mainly from SCISRS and NEUDADA files by the request to CCDN, and the other data have been obtained by usrveying published reports or by private communications. These data are from 1946 to 1970 inclusive. These collected data are compiled and stored in magnetic tape for computer calculation.

Characteristics of the individual data set are shown in Fig. 1. The energy ranges covered by these data sets are shown with solid and dashed lines. The colid lines indicate the data sets obtained by the method of time-of-flight (TOF), and the dashed lines indicate those obtained by the method of direct-current-beam (DCB). In the present report, the TOF data mean those obtained with incident neutrons of continuous spectrum. Those data obtained with incident neutrons from a monoenergetic neutron source are defined as DCB data, even if TOF technique is used in some cases.

Numerical values in the 1st, 2nd and 3rd parentheses of Fig. 1 represent the number of data points, percent errors and reference numbers. Seven references[15-17),21)24),26),43)] are not shown in Fig. 1, since each of them includes only one to four data points (see Table I).

The energy region of interest is from 1 eV to 2 MeV, in which the number of references surveyed is 32. The contents of 32 references[6-8),15-43)] surveyed are summarized in Table I according to those specific items such as authors, laboratory, year, energy range, number of data points, errors, method, sample and remarks. Detailed characteristic items of the individual data set are not always given in the original paper. For such a case, the answers from the individual authors for questionnaire are most helpful for getting necessary information in order to fill up the items in Table I.

Due to the addition of newly obtained data at the later stage of this work, the number of data points in Data Set No. 2 increased remarkably compared with those of Data Set No. 1. The contents of newly added data in Data Set No. 2 are listed in Table II, as well as those of Data Set No. 1.

2) Data representation

The total number of data points collected for the present evaluation amounts to 8,241 in the energy region of interest. The data sets with many data points are as follows:

109 points from ANL (Hibdon),

624 points from Duke (Seth et al.),

997 points from ANL (Whalen et al.),

2070 points from NBS (Schwarz et al.),

660 points from ANL (Huddleston et al.),

2118 points from KFK (Cierjacks et al.),

427 points from RPI (Yergin et al.).

By using a calcomp plotter, these cross-section values in Data Set No. 1 and Data Set No. 2 are plotted in Fig. 2 and Fig. 3, respectively.

According to the method of measurement, those data shown in Fig. 2 are classified into TOF and DCB data, and they are plotted with the marks of ⏀ and △. In order to clarify the dense part of the data points in Fig. 3, an enlarged scale of neutron energy is adopted in Figs. 4 to 10, where classification into TOF and DCB data is also made. The TOF data in Fig. 3 are plotted in Figs. of 4, 5 and 6, corresponding to the energy range of 100 keV - 600 keV, 0.6 MeV - 1.2 MeV, and 1.2 MeV - 2.0 MeV, respectively. The DCB data in Fig. 3 are plotted in Figs. of 7, 8 and 9, corresponding to the same energy range as in Fig. 3. Futhermore, the most dense parts of the DCB data in Figs. 7 and 8 are shown in Fig. 10 in the energy range of 500 keV - 700 keV.

## 3. Method of evaluation

So far as the existing experimental data are investigated, it is concluded that the neutron total cross section of carbon in the energy region of 1 eV to 2 MeV has no resonance structure and can be represented with sufficient accuracy by a slowly varying smooth function of energy. As is shown in Appendix A, it is shown theoretically that the cross section in the region sufficiently far-off from the resonances can be reasonably expressed by a polynomial of energy. Therefore, the polynomial equation is adopted as an empirical formula in the present paper to express the recommended value of the total cross section of carbon in question. In order to obtain an empirical formula, a polynomial is fitted to the experimental data points by the least-squares method. A note on the least-squares method is given in Appendix B.

A polynomial of a lower order is desirable from practical view-point as far as the accuracy of the representation by the obtained polynomial is sufficient in comparison with an expected accuracy of the experimental data. A fourth order polynomial is adopted in conclusion after a practical examination which is described in the following section. This adoption is compatible with those empirical formulae of second to fourth order polynomials obtained by other investigators[6-10], and facilitates the comparison with those formulae.

On the assumption that the cross section is a smooth function of the energy and has no fine structure, a small number of data points scattered from the majority of the data points are allowed to be rejected from the data set to which the least-squares fit of a polynomial is made. Actual method of the rejection is mentioned in the following section.

To begin with the least-squares fit to obtain an empirical formula as the most plausible representation of the experimental data points, a weight to be imposed on each data point should be considered. This is one

of the most important problem in the evaluation work, especially in the case where the data sets of different qualities in accuracy are treated; the method to evaluate a proper weight is not simple since the reported information on the accuracy is generally not sufficient to treat the problem quantitatively.

Errors of an experimental data point of the total cross section can be classified into 1) statistical error $\Delta\sigma_{st}$ from the error of the various counts: open beam count, sample-in count, background counts, and monitor count, 2) other accidental error $\Delta\sigma_{ac}$ which should include errors of sample thickness and corrections, if any, and 3) error of the unknown factor which might include systematic error not corrected by the experimenter. The error of the third type cannot be incorporated in the general procedure of the evaluation work, and only in an exceptional case, the magnitude of it could be estimated after an evaluation.

First, we consider only one data set of an experiment in a narrow energy region where the cross section is effectively constant, and write the experimental data and their errors as follows:

$$\sigma_{exp,i} \pm \Delta\sigma_{exp,i} \quad , \quad i = 1, 2, 3, \ldots\ldots N,$$

and

$$(\Delta\sigma_{exp,i})^2 = (\Delta\sigma_{st,i})^2 + (\Delta\sigma_{ac})^2,$$

although $\Delta\sigma_{ac}$ may not strictly conform to the Gaussian law. A simple mathematical mean of the N data points may be written as

$$\frac{\sum_{i=1}^{N} \sigma_{exp,i}}{N} \pm \left\{ (\Delta\sigma_{ac})^2 + \frac{\sum_{i=1}^{N} (\Delta\sigma_{st,i})^2}{N^2} \right\}^{1/2}$$

Next, we consider more than one data set of independent experiments, and

the experimental errors

$$(\Delta\sigma_{exp,ij})^2 = (\Delta\sigma_{st,ij})^2 + (\Delta\sigma_{ac,j})^2, \qquad (3\text{-}1)$$

$$i = 1, 2, \ldots\ldots, N_j,$$

$$j = 1, 2, \ldots\ldots, M,$$

where $N_j$ is the number of the data points in the set j and M the number of different sets. If we suppose an effective error $\Delta\sigma_{eff,ij}$ which satisfies the following equation:

$$(\Delta\sigma_{ac,j})^2 + \frac{\sum_{i=1}^{N_j}(\Delta\sigma_{st,ij})^2}{N_j^2} = \frac{\sum_{i=1}^{N_j}(\Delta\sigma_{eff,ij})^2}{N_j^2},$$

hence

$$(\Delta\sigma_{eff,ij})^2 = N_j(\Delta\sigma_{ac,j})^2 + (\Delta\sigma_{st,ij})^2 ,$$

then the weight $W_{ij}$ to be assigned to each point to calculate an averaged value of all points in M sets may be taken to be

$$W_{ij} = \frac{1}{(\Delta\sigma_{eff,ij})^2} = \frac{1}{(\Delta\sigma_{st,ij})^2 + N_j(\Delta\sigma_{ac,\,j})^2}. \qquad (3\text{-}2)$$

Difficulty in actuality is, however, that the relation like Eq.(3-1) is not generally clear for the experimental errors given in the literature: only the error from the counting statistics is given in a literature, or it is not clear in another literature whether an error given to the data point is a combined one of the discussed errors or not, and so forth.

If $(\Delta\sigma_{st,ij})^2 > N(\Delta\sigma_{ac,j})^2$ and $\Delta\sigma_{exp,ij} \simeq \Delta\sigma_{st,ij}$, then $W_{ij}$ of the expression (3-2) results in $W_{ij} \simeq 1/(\Delta\sigma_{exp,ij})^2$; and if $\Delta\sigma_{st,ij} < \Delta\sigma_{ac,j}$ and $\Delta\sigma_{exp,ij} \simeq \Delta\sigma_{ac,j}$, then $W_{ij} \simeq 1/N_j(\Delta\sigma_{exp,ij})^2$.

Since

$$\frac{1}{N_j(\Delta\sigma_{exp,ij})^2} \leq W_{ij} \leq \frac{1}{(\Delta\sigma_{exp,ij})^2},$$

we adopt the following expression of the weight $W_{ij}$ to the data point (ij) in our least-squares fit:

$$W_{ij} = a_j \frac{1}{f(N_j)} \cdot \frac{1}{(\Delta\sigma_{exp,ij})^2} \qquad (3\text{-}3),$$

where $f(N_j)$ is a function of $N_j$, $1 \leq f(N_j) \leq N_j$, and $a_j$ a weight factor assessed to the set j by the evaluator. The functional form of $f(N_j)$ should be different among the different data sets, but it is unknown practically, and in the following least-squares fits, one functional form of $f(N_j)$ is taken in a fit: $f(N_j) = 1$, $\sqrt{N_j}$, or $N_j$.

In the above discussion, the distribution of the data point over the neutron energy is neglected. Since an assessment of $a_j$ in comparison with different data sets in different energy regions is difficult, a weight $W_{ij}$ should be assessed in a relatively narrow energy region:

$$W_{ij} = a_{je} \frac{1}{f(N_{je})} \cdot \frac{1}{(\Delta\sigma_{exp,ij})^2}, \qquad (3\text{-}4)$$

where $a_{je}$ is an evaluator's weight factor for the set j in the energy region e. This assessment is also not straightforward in practice, and in the following, a simple test with $a_{je}=a_j$ is made. In this case, $W_{ij}$ of Eq.(3-4) is larger than or equal to $W_{ij}$ of Eq.(3-3).

Although a combined error $\Delta\sigma_{exp,ij}$ should be assessed to the data point when the single point is considered, it is, in the sense of Eq.(3-2), recommended to the experimenters that only the error from the counting statistics should be attached to the individual data point and the error of the other type should be described separately. This may have already been put into practice by many experimenters, but it would be worthy to mention since it is not always clear in the publications.

## 4. Procedure and results

Calculations of least-squares fit to the experimental data (Data Set No. 1) were tried using third order to fifth order polynomials. Results of the three polynomials were compared with each other, and little difference was found among them except for the energy region near 2.0 MeV. Differences between the results of the third and fifth order polynomials were as follows; less than 0.25 % in the energy region below 10 keV, less than 0.2 % between 10 keV and 100 keV, less than 1 % between 100 keV and 1 MeV, less than 0.7 % between 1 MeV and 1.5 MeV, less than 1 to 1.5 % between 1.5 and 1.9 MeV, and about 5 % near 2 MeV. The differences between fourth and fifth order polynomials were found about a half or one-third less than the difference between the results of third and fifth order polynomials. Thus, a fourth order polynomials is chosen to represent the cross section in this work, i.e.

$$\sigma_{nT}(E) = a_0 + a_1E + a_2E^2 + a_3E^3 + a_4E^4 \ . \qquad (4\text{-}1)$$

There are some data points deviating anomalously from the majority. Before doing the calculation, these data points have to be rejected, provided that there is no structural variation in the cross section. A measure of the anomalous deviation is defined as follows. A cross-section curve is calculated by the least-squares method applied to all the data points with equal weight. Deviation of the data points from the cross-section curve is defined as

$$\varepsilon^2 = \frac{(\sigma^i_{exp} - \sigma^i_{cal})^2}{N - 5} \ , \qquad (4\text{-}2)$$

where $\sigma^i_{exp}$ is the experimental cross section at the i-th energy point, $\sigma^i_{cal}$ is the calculated value at the same energy, and N is the number of data points. Quantity $\varepsilon^2$ is the stnadard deviation for the case of equal weight. An adopted criterion for the rejection is

$$(\sigma^i_{exp} - \sigma^i_{cal})^2 > 10\varepsilon^2. \qquad (4\text{-}3)$$

Empirical formulae which will be shown in the following are all derived from the data points which do not exceed this criterion.

The coefficients of $a_i$ (i=0, 1, 2, 3, 4) in Eq.(1) are deduced from the fitting of the cross section data by the least-squares method. In the calculations, the following steps have been taken into account in the assignment of weights to the experimental data points;

(1) equal weight,

(2) weight of $1/(\Delta\sigma_i)^2$

(3) weight of $a_j/f(N_j)(\Delta\sigma_{ij})^2$.

Here, $\Delta\sigma_{ij}$(or $\Delta\sigma_i$) and $N_j$ are experimental errors and the number of data points in a specific data set j, respectively;and the functional form is taken as f=1, $f=\sqrt{N_j}$ or $f=N_j$. The factor $a_j$ is a weight assigned by the present authors to the specific data set j.

In the case of (1) and (2), calculations were performed for the Data Set No. 1 in the energy region from 1 eV to 2 MeV. The results are shown in the following;

$$\sigma_{nT}(E) = 4.729 - 2.968E + 0.551E^2 + 0.413E^3 - 0.166E^4 \quad \text{for equal weight,} \quad (4\text{-}4)$$

and

$$\sigma_{nT}(E) = 4.736 - 3.109E + 0.855E^2 + 0.162E^3 - 0.097E^4 \quad \text{for } (1/\Delta\sigma)^2. \quad (4\text{-}5)$$

In the case that no information of errors is available from the original papers, their errors $\Delta\sigma_i/\sigma_i$ are tentatively assigned to be 5 %. A similar calculation with the error assignment of 10 % for the data having no description of errors is also performed. The results indicated that the values of the corresponding coefficients in the two polynomials obtained are same within ± 2 in the fourth digit. This is considered to be reasonable from the fact that the number of data points with no description of errors

is less than 300, which is small compared with the total number of data points, and that the error of 5 % assigned to them is not so small compared with the other original errors, which are typically 2 to 4 %. In the case of the weight $(1/\Delta\sigma_i)^2$, the result of the cross section-curve of Eq.(4-5) is shown by a solid curve in Fig. 2.

In order to find out systematic difference due to the experimental method, the least-squares analyses are also applied to both DCB and TOF data separately in the case of (1) and (2). There are scarecely any DCB data below 1 keV, so that the energy region compared is 1 keV to 2 MeV. The results are shown in the following:

$$\sigma_{nT}(E) = 4.841 - 3.792E + 2.333E^2 - 0.976E^3 + 0.184E^4$$
for equal weight and DCB, (4-6)

$$\sigma_{nT}(E) = 4.740 - 3.013E + 2.934E^2 - 1.306E^3 + 0.234E^4$$
for equal weight and TOF, (4-7)

$$\sigma_{nT}(E) = 4.866 - 3.892E + 2.515E^2 - 1.106E^3 + 0.214E^4$$
for $(1/\Delta\sigma)^2$ and DCB, (4-8)

$$\sigma_{nT}(E) = 4.739 - 3.537E + 1.706E^2 - 0.384E^3 + 0.017E^4$$
for $(1/\Delta\sigma)^2$ and TOF. (4-9)

These results had been obtained by April 1970. After that, many data sets were newly added to NEUDADA and were included in the input data for the following least-squares analyses.

In the case of (3), that is the case of the weight factor $a_j/f(N_j)(\Delta\sigma_{ij})^2$, more reasonable assessment of the weight is taken into account for Data Set No. 2. The factor $a_j$, mentioned above, is chosen to reflect such characteristic items of the individual references as those summarized in Table 1.

The following items should be considered to assess the weight factor $a_j$, when ideal evaluation is performed.

i) It may be more probable that data set with lower experimental error has

lower unknown systematic error.

ii) A higher weight may be assigned to the data set from the experiment of which original purpose is to obtain a precise value of the cross section, and on the contrary, if the original purpose of the measurement is a check of the method of background determination, for example, a lower weight may be assigned to the data.

iii) A low weight is assigned to the data set of the report with no original error assessment to the data or with insufficient description of the experimental condition.

iv) If the year of publication of the data is old, a relatively low weight may be assigned to the data.

A quantitative assessment of the weight factor $a_j$ is, actually, not straightforward; and in the present evaluation, the value of $a_j$=0, 0.5 or 1.0 is simply assigned to the individual data set by laying down the following criteria:

a) $a_j$=0 is assigned to the data set in which the errors larger than 3 % were assessed to the individual data points or no description of the error was made by the original authors. In other words, those data sets are not adopted as the input data for making the least-squares fit to obtain the empirical cross-section formula in the present evaluation.

b) For the data set with the errors less than 3 %, $a_j$=0.5 is assigned to the data set published before 1955, and $a_j$=1.0 is given otherwise.

The results of the least-squares fit to the data points of 7,758 with the three kinds of weights $W_{ij}$, discussed in the previous section, are as follows:

$$\sigma_{nT}(E) = 4.697 - 3.080E + 1.235E^2 - 0.273E^3 + 0.025E^4$$

$$\text{for } W_{ij} = a_j/(\Delta\sigma_{ij})^2 \qquad (4\text{-}10)$$

$$\sigma_{nT}(E) = 4.699 - 3.061E + 1.069E^2 - 0.095E^3 - 0.026E^4,$$
$$\text{for } W_{ij} = a_j/\sqrt{N_j}(\Delta\sigma_{ij})^2 \quad (4\text{-}11)$$

$$\sigma_{nT}(E) = 4.705 - 3.018E + 0.862E^2 + 0.082E^3 - 0.068E^4,$$
$$\text{for } W_{ij} = a_j/N_j(\Delta\sigma_{ij})^2 \quad (4\text{-}12)$$

The cross-section curves are shown in Fig. 11.

As mentioned above, the weight factor $a_j$ of zero is given to the data sets having no description of errors or having the errors larger than 3 %, and these data are not accepted as the input data for the fitting calculation. To check the effect of this elimination of the data, the least-squares calculation has been performed with the same procedure as in the case of $W_{ij} = a_j/\sqrt{N_j}(\Delta\sigma_{ij})^2$, including those eliminated data with an assumed error of 5% to each data point. The result is the following:

$$\sigma_{nT}(E) = 4.699 - 3.052E + 1.031E^2 - 0.062E^3 - 0.034E^4. \quad (4\text{-}11')$$

No significant difference between Eq.(4-11) and Eq.(4-11') is seen. This gives a passive support to the present elimination of the data sets.

The same procedure of the least-squares fitting with the weight of $W_{ij} = a_j/\sqrt{N_j}(\Delta\sigma_{ij})^2$ is applied to both DCB and TOF data, separately. The difference between their results are shown in Fig. 12 and the polynomial expressions obtained in the whole region from 1 eV to 2 MeV are written as follows:

$$\sigma_{nT}(E) = 4.695 - 2.853E + 0.442E^2 + 0.465E^3 - 0.180E^4 \text{ for DCB} \quad (4\text{-}13),$$

$$\sigma_{nT}(E) = 4.752 - 3.769E + 2.596E^2 - 1.208E^3 + 0.236E^4 \text{ for TOF} \quad (4\text{-}14).$$

## 5. Discussions

### 1) Difference between the results with the three kinds of weight

According to the consideration on the weights in Section 3, the weights $W_{ij}=a_j/(\Delta\sigma_{ij})^2$ and $W_{ij}=a_j/N_j(\Delta\sigma_{ij})^2$ correspond to the cases $\Delta\sigma_{exp,ij}\simeq\Delta\sigma_{st,ij}$ and $\Delta\sigma_{exp,ij}\simeq\Delta\sigma_{ac,j}$, respectively, and they are the two extremes in the weight to be considered. The experimental errors will be the combination of $\Delta\sigma_{st,ij}$ and $\Delta\sigma_{ac,ij}$, but the magnitude of $\Delta\sigma_{ac,ij}$ is unknown in many cases. On the other hand, the value of the weight $a_j/\sqrt{N_j}(\Delta\sigma_{ij})^2$ is between those for $W_{ij}=a_j/(\Delta\sigma_{ij})^2$ and $W_{ij}=a_j/N_j(\Delta\sigma_{ij})^2$. In this respect, one may expect that the weight $a_j/\sqrt{N_j}(\Delta\sigma_{ij})^2$ results in better cross-section values than those obtained with the other two extremes. As expected from the above consideration, Fig. 11 shows that the cross-section curve for $W_{ij}=a_j/\sqrt{N_j}(\Delta\sigma_{ij})^2$ lies between the other two curves.

In the above discussion, the effect of the non-uniform distribution of the data points over the neutron energy is not taken into account. As was already pointed out in Section 3, a rigorous account of this effect is very difficult. For convenience, the whole energy region is divided into a certain number of sub-regions, and the least-squares fits with the weights $W_{ij}=a_{je}/f(N_{je})(\Delta\sigma_{ij})^2$ are tried in order to see this effect. (See Eq.(3-4)) Practically, the following two cases are tried: First, the whole energy region is divided into 13 sub-regions, where about 600 data points are included in every sub-region. The boundary values of the energy sub-regions are 1 eV, 480 keV, 580 keV, 665 keV, 795 keV, 1.01 MeV, 1.125 MeV, 1.22 MeV, 1.375 MeV, 1.65 MeV, 1.80 MeV and 2.0 MeV. The results are shown in Fig. 13. Secondly, the whole region is divided into 5 sub-regions. The boundary values are 1 eV, 480 keV, 745 keV, 1.0 MeV, 1.57 MeV and 2.0 MeV, and the results are shown in Fig. 14.

Fig. 15 shows the differences between the curves with and without the

division of the energy region in the cases of weights $a_{je}/\sqrt{N}_{je}(\Delta\sigma_{ij})^2$ (dashed line) and $a_{je}/N_{je}(\Delta\sigma_{ij})^2$ (solid line). Notice that the differences are plotted on an expanded scale.

It is seen that there is no remarkable difference in the cross-section values with the weights of Eq.(3-3) and Eq.(3-4), as far as the present division of the energy regions is concerned. Especially, the differences among the three curves with the weight $a_{je}/\sqrt{N}_{je}(\Delta\sigma_{ij})^2$ are usually smaller than the differences among those for the weight $a_{je}/N_{je}(\Delta\sigma_{ij})^2$.

2) Comparison between the cross-section curves obtained with Data Set No. 1 and Data Set No. 2

In order to see the difference in the cross-section values caused by the different data sets, i.e. Data Set No. 1 and Data Set No. 2, the least-squares fit was also made for Data Set No. 1 with the weight $W_{ij}=a_j/\sqrt{N}_j(\Delta\sigma_{ij})^2$, and the following equation was obtained:

$$\sigma_{nT}(E) = 4.733 - 3.182E + 0.950E^2 + 0.133E^3 - 0.097E^4. \qquad (5\text{-}1)$$

In Fig. 16, the cross-section curve from this equation (dotted curve) is compared with the corresponding curve obtained with Data Set No. 2 (dashed curve from Eq.(4-11)). A large difference is seen in the energy region of 0.7 to 1.4 MeV. The larger value of the dashed curve than the dotted one in this energy region is mainly caused by the contribution of two data sets of Huddleston et al.[6] and Cierjacks et al.[39], which were newly added in Data Set No. 2.

3) Difference between the TOF and DCB data

In order to check any possible systematic differences between the sets of data taken with different experimental methods, all the data sets considered here are classified into the time-of-flight (TOF) data and the direct-current beam (DCB) data according to the technique of measurement. In the present work, the data, which were obtained with incident neutrons

of continuous spectrum and by using the time-of-flight technique to analyze the neutron energy, are classified into the TOF data. They are usually obtained using a linear accelerator or sometimes using a cyclotron. On the other hand, the data obtained with incident neutrons from a monoenergetic neutron source are classified into the DCB data, even if the time-of-flight technique was also employed in some cases. These data are usually obtained using a Van de Graaff accelerator. One will expect a general trend that the TOF method is favorable in determining the whole shape of the cross-section curve in a large energy range, and the DCB method is suitable for the determination of the absolute values of the cross sections, although the number of the data points is usually meager.

The differences between the results of the least-squares fitting applied to the TOF and DCB data are shown in Fig. 12 by a dotted line for the $a_j/(\Delta\sigma_{ij})^2$ treatment (Eq.(4-8)-Eq.(4-9)) and by a solid line for the $a_j/\sqrt{N_j}(\Delta\sigma_{ij})^2$ treatment (Eq.(4-13)-Eq.(4-14)). One may easily notice that there are considerably different features between these two results: (1) The solid curve is more oscillatory than the dotted curve: (2) The signs of the solid curve and the dotted curve are almost opposite to each other in the energy range above 0.7 MeV: (3) The solid curve is negative in the energy range less than 90 keV. These different features are mainly caused by the contribution of several data sets which were newly employed or rejected as $a_j=0$ in the $a_j/\sqrt{N_j}(\Delta\sigma_{ij})^2$ treatment rather than by the difference of the weights between the two results. For example, the fact that the solid curve is negative in the energy region less than 90 keV is mainly caused by the rejection of the data sets with large cross-section values such as Hibdon's data in the $a_j/\sqrt{N_j}(\Delta\sigma_{ij})^2$ treatment. Therefore, the scatter of the cross-section values among the different data sets makes ambiguous the small systematic difference between the TOF and DCB data, if any.

4) Cross Sections below 1 keV

At thermal and epithermal energies, absolute values of the total cross sections were reported in several articles. They are 4.66 ± 0.03 b (graphite sample) and 4.74 ± 0.06 b (diamond-dust sample) at $E_n$=1.44 eV[17]; 4.77 ± 0.05 b at $E_n \simeq 0.025$ eV[15),44)]; 4.743 ± 0.002 b at $E_n$=33.9 eV[21)]; 4.7264 ± 0.0024 b at $E_n$=61.1 eV[21)]; and 4.7534 ± 0.0045 b in the energy range of 0.3 to 400 eV[15)]. These data points are shown in Fig. 17.

Recently, a TOF measurement was made at Harwell[8)] from 74 eV to 1.56 MeV, and a fourth order polynomial, which is given by Eq.(5-4) in the following subsection, was fitted to their data: The lower part of the fitted curve is shown by a dashed line in Fig. 17 for comparison.

As is seen in Fig. 17, the cross-section value in the present work is smaller than the values in the above except for one data point. However, because of the large scatter and the small number of the available data points, it is quite difficult to discuss the cross-section values adequately in this energy region.

5) Comparison with results of other authors

In Fig. 18, the present cross section curve with the weight of $W_{ij}=a_j \sqrt{N_j}(\Delta\sigma_{ij})^2$ is compared with the cross section curves of other authors:

$$\sigma_{nT}(E) = 4.710 - 3.415E + 1.649E^2 - 0.2606E^4, \quad (5\text{-}2)$$

by Huddleston et al.[6)] in the energy range 0.50 ∿ 1.35 MeV,

$$\sigma_{nT}(E) = 4.95 - 4.24E + 2.23E^2 \quad (5\text{-}3)$$

by Seth et al.[7)] in the energy range 3 ∿ 660 keV,

$$\sigma_{nT}(E) = 4.744 - 3.707E + 2.389E^2 - 1.114E^3 + 0.242E^4 \quad (5\text{-}4)$$

by Uttley and Diment[8)] in the energy range less than 1.56 MeV, and

$$\sigma_{nT}(E) = 4.830 - 3.55E + 1.587E^2 - 0.305E^3 \quad (5\text{-}5)$$

by Meadows and Whalen[9)] in the energy range 0.1 ∿ 1.5 MeV,

$$\sigma_{nT}(E) = 4.513 - 2.343E + 0.465E^2 + 0.012E^3 \quad (5\text{-}6)$$

by Ahmed et al.[10] in the energy range 0.5 ∿ 2 MeV.
These polynomials were obtained by the other authors by being fitted to their own measured cross sections. Most of these measurements were made using the transmission method. Only Ahmed et al. obtained the total cross sections from measured scattering cross sections by integration with making use of the fact that the (n,γ) cross-section value is neglegibly small. Their results were not included in the present work. The curve of Meadows and Whalen almost coincides with the curve of Uttley and Diment in the energy range from 0.7 to 1.6 MeV.

The present cross section curve is compared further with those of BNL 325[2], ENDF/B[13], KFK 750[3] and AWRE[4),11] data files. These cross section curves in the energy regions of eV, keV and MeV are shown in Fig. 19, Fig. 20, and Fig. 21, respectively. The agreement of KFK 750 curve with the present one is rather good than that of the others below 700 keV. In Fig. 19 and Fig. 20, the deviation of BNL 325 and ENDF/B curves from the present one is remarkable below 200 keV. The large values of those curves in the lower energy region is mainly caused by that the large cross section values of Seth et al. were used to obtain those curves. AWRE curve and KFK 750 curve coincide with each other and the values of those curves are quite large around 1 MeV. This is because the data in those files were obtained by using Huddleston's formula in this energy region, which shows large values as seen in Fig. 18. In the energy region higher than 1.4 MeV, AWRE data curve considerably deviates from the rest of the curves towards lower value. According to the AWRE report, the author obtained this part of the curve from several data sets available at that time. It is supposed that the values in those data sets would be comparatively small.

6) Uncertainty of the present cross-section curve

The width of the confidence band (see Appendix B) calculated at 95 %

confidence level for the present cross-section curve in the case of the weight, $W_{ij}=a_j/\sqrt{N_j}(\Delta\sigma_{ij})^2$ is less than ± 10 mb below $E_n$=1.8 MeV and becomes a little larger value of about ± 20 mb at $E_n$=2 MeV. These values are quite small and amount only 1 % at most of the magnitude of the cross section. They are obtained, however, under the assumption that each error assigned to the data point can be treated statistically. Besides, there will be systematic error, and this cannot be treated analytically. As far as the present work is concerned, only the difference between the TOF and DCB cross-section curves will reflect the magnitude of the systematic error, although the difference between the present and Ahmed's curves might give also a measure relevant to the systematic error. The difference between the TOF and DCB curves is about 2 % of the cross-section value and the difference between the present and Ahmed's curves is 2 to 3 % in the energy range less than 1.8 MeV. Therefore, it is likely that the present cross-section curve will have an uncertainty less than 2 to 3 % of the cross-section value.

As for the uncertainty in the energy region near 2 MeV, a large number of data points in the lower energy region might affect the evaluated cross-section value in this energy region, because the number of the data points near 2 MeV is rather rare and no data point in the energy region higher than 2 MeV was employed in the present work. Actually this effect appears as the broadening of the calculated confidence band, and as a large difference between the TOF and DCB curves. Moreover, owing to the fact that the energy region near 2 MeV is very close to the large 2.076-MeV resonance peak, the procedure of the fourth order polynomial fitting might lead to an evaluated value with large error in this energy region (see Appendix A). For these reasons, the uncertainty of the present cross-section value in the energy region higher than 1.8 MeV should be enlarged more than 3 % of the cross-section value in a practical use.

## 6. Conclusion and remark

As was already discussed, there is no definite reason why one should choose $\sqrt{N_j}$ as the functional form of $f(N_j)$ in the equation for the weight $W_{ij}=a_j/f(N_j)(\Delta\sigma_{ij})^2$. Nevertheless, in the present work $\sqrt{N_j}$ is chosen because of the following two evidences: (1) The weight $W_{ij}=a_j/\sqrt{N_j}(\Delta\sigma_{ij})^2$ gives medium values between the values of $W_{ij}=a_j/(\Delta\sigma_{ij})^2$ and $W_{ij}=a_j/N_j(\Delta\sigma_{ij})^2$, which are the two extremes in the weight to be considered. (2) The cross-section values obtained from Eq.(4-11) show medium values between those of Eq.(4-10) and Eq.(4-12), while the difference between the values of Eq.(4-10) and Eq.(4-12) is not large.

In conclusion, for the total neutron cross section of carbon in the energy range from about 1 eV to 2 MeV, we recommend the empirical formula Eq.(4-11):

$$\sigma_{nT} = 4.699 - 3.061E + 1.069E^2 - 0.095E^3 - 0.026E^4,$$

where $\sigma_{nT}$ is in barns and E in MeV. For convenience of practical use, the values calculated with this formula are listed in Table III. As discussed at the end of the preceding section, the uncertainty of these cross-section values are less than 2 to 3 % in the energy region up to 1.8 MeV, and above this energy the uncertainty should be enlarged more than 3 %.

As seen from comparison between Fig. 2 and Fig. 3, some data sets in Data Set No. 2 were rejected by the criterion of $a_j=0$, hence there remain only a few data sets in the energy region less than 100 keV. Moreover, there are rather large differences in cross-section values among the different data sets in the energy region of 5 $\sim$ 100 keV. Therefore, it is desirable that in the near future highly reliable experimental data will be added to available data sets in the energy region less than 100 keV.

Acknowledgements

The authors are indebted to Professor T. Momota for his suggestions and interest in this work. We would like to express our gratitude to Dr. K. Tsukada and Professor R. Nakasima for helpful and stimulating discussions. The authors are also grateful to Drs. K. Parker, J. J. Schmidt, S. Schwarz, L. Stewart and R. F. Taschek for useful comments in the early stage of this evaluation work. Kind responses from individual experimenters for questionnaire are most helpful, and we take pleasure in acknowledging them for getting detailed information. Finally, thanks are due to the stuff members of CCDN for providing us a large number of experimental data available for this study.

## References


1) Complete Minutes of the 8th Meeting of the EANDC: Los Alamos, 17-21 May, 1965

IAEA-107 (Dec. 1968); Report of the Panel on Nuclear Standards needed for Neutron Cross Section Measurements: Brussels, 8-12 May, 1967

EANDC Symposium on Neutron Standards and Flux Normalization: Argonne, 21-23 Oct., 1970

2) BNL 325, 2nd Edition, Supplement No. 2 Neutron Cross Sections, Vol. 1 (1964)

3) Langner I., Schmidt J. J., Woll D., KFK 750, Tables of Evaluated Neutron Cross Sections for Fast Reactor Materials, (1968)

4) Parker K.: AWRE Report No. 071/60

5) BNL 400, 2nd Edition, Angular Distributions in Neutron-Induced Reactions, Vol. 1 (1962)

6) Huddleston C. H., Lane R. O., Lee Jr., L. L. and Mooring F. P.: Phys. Rev. 117, 1055 (1960)

7) Seth K. K., Bilpuch E. G. and Newson H. W.: Nucl. Phys. 47, 137 (1963)

8) Uttley C. A. and Diment K. M., EANDC(UK) 94"AL" (1968); Helsinki Conf. IAEA, CN-26/24 (1970).

9) Meadows J. W. and Whalen J. F.: private communication (1970)

10) Ahmed N., Coppola M., Knitter H. H.: Helsinki Conf. IAEA, CN-26/23 (1970)

11) Barrington E. P., Pope A. L., Story J. S.: AEEW R-351 (1964)

12) Schmidt J. J.: KFK-120, EANDC(E)-35"U" (1966)

13) Slaggie E. L., Reynolds J. T.: KAPL 3099 (1966)

14) Nishimura K., Igarasi S., Fuketa T. and Tanaka S.:JAERI-memo 3884 (1970)

15) Walton R. B., Wikner N. F., Wood J. L. and Beyster J. R.: Bull. Am. Phys. Soc. 5, 288 (1960)

16) Houk T. L. and Wilson R.: Rev. Mod. Phys. 39, 546 (1967)

17) Rayburn L. A. and Wollan E. O.: Nucl. Phys. 61, 381 (1965)

18) Egelstaff P. A.: Private communication to SCISRS, data of (1952)

19) Simpson O. D., Fluharty R. G. Moore M. S. Marshall N. H. Simpson F. B. Stokes, G. E. Watanabe T. and Young T. E.: Nucl. Inst. Meth. 30, 293 (1964)

20) Brugger R. M., Evans J. E., Joki E. G. and Shankland R. S.: Phys. Rev. 104, 1054 (1956)

21) Triftschäuser W. and Fehsenfeld P.: EANDC(E)-57"U" 21 (1965)

22) Hibdon C. T.: Private communication to SCISRS, data of (1954)

23) Mooring F. P., Monahan J. E. and Huddleston C. M.: Nucl. Phys. 82, 16 (1966)

24) Miller D. W.: Phys. Rev. 78, 806 (1950)

25) Fields R., Russell B., Sacks D. and Wattenberg A.: Phys. Rev. 71, 508 (1947)

26) Frisch D. H.: Phys. Rev. 70, 589 (1946)

27) Kiehn R. M., Goodman C. and Hansen K. F.: Phys. Rev. 91, 66 (1953)

28) Allen W. D. and Ferguson A. T. G.: Proc. Phys. Soc. (London) A68, 1077 (1955)

29) Whalen J. F. et al.(1): Private communication (1967)

30) Cance M., Cabe J., Adam A., Beaufour M. and Labat M.: GF N° 187/W (1970)

31) Wilenzick R. M., Mitchell G. E., Seth K. K. and Lewis H. W.: Phys. Rev. 121, 1150 (1961)

32) Bretscher E. and Martin E. B.: Helv. Phys. Acta. 23, 15 (1950)

33) Bailey C. L., Bennett W. E., Bergstralh T., Nuckllos R. G., Richards H. T. and Williams J. H.: Phys. Rev. 70, 583 (1946)

34) Schwarz R. B., Heaton II H. T. and Schrack R. A.: Bull. Amer. Phys. Soc. 15, 567 (1970)

35) Freier G., Fulk M., Lampi E. E. and Williams J. H.: Phys. Rev. 78, 508 (1950)

36) Smith A. B. and Whalen J. F.: Private communication (1969)

37) Cabe J., Laurat M. and Yvon P.: EANDC(E)-49"L" 69 (1963)

38) Whalen J. F. et al. (2): Private communication (1969)

39) Cierjacks S., Forti P., Kopsch D., Kropp L. and Neve J.: Second Conference on Neutron Cross Sections and Technology, Vol. 2, 743 (1968)

40) Yergin P. F., Martin R. C., Winhold E. J., Medicus H. A., Moyer W. R., Augustson R. H., Kaushal N. N. and Fullwood R. R.: Neutron Cro , Section Technology, Vol. 2, 690 (1966)

41) Lampi E. E., Freier G. D. and Williams J. H.: Phys. Rev. 80, 853 (1950)

42) Bockelman C. K., Miller D. W., Adair R. K. and Barshall H. H.: Phys. Rev., 84, 69 (1951)

43) Storrs C. L. and Frisch D. H.: Phys. Rev. 95, 1252 (1954)

44) Uttley C. A. and Diment K. M.: AERE-PR/NP 13, p. 4 (1968)

Appendix A.

Neutron total cross section is generally written as follows;

$$\sigma_{nT}(E) = \frac{2\pi}{k^2} \Sigma_{J\Pi s\ell} g^J \mathrm{Re}(1 - U^{J\Pi}_{s\ell;s\ell}) \quad , \tag{A-1}$$

where k is the wave number, $g^J$ is the statistical weight factor. Diagonal element of collision matrix, $U^{J\Pi}_{s\ell;s\ell}$, is given by the formula

$$U^{J\Pi}_{s\ell;s\ell} = e^{2i\Omega_\ell}\left\{1 + i\sum_\lambda \frac{\Gamma_{\lambda s\ell}}{E_\lambda - E - \frac{1}{2} i\Gamma_\lambda}\right\} , \tag{A-2}$$

provided that all resonances are isolated. In the energy region far from the resonances, main dependence on the energy comes from $\exp(2i\Omega_\ell)$. Resonance terms contribute only through the penetration factors in the level width $\Gamma_{\lambda s\ell}$ and $\Gamma_\lambda$. Assuming $\Gamma_\lambda \simeq \Gamma_{\lambda s\ell}$,

$$\mathrm{Re}(1 - U^{J\Pi}_{s\ell;s\ell}) = 1 - (1 - a_\ell \rho^2 v_\ell^2) v_\ell (G_\ell^2 - F_\ell^2) - 2b_\ell \rho v_\ell^2 F_\ell G_\ell , \tag{A-3}$$

where $\rho = kR$, R is the nuclear radius. Functions $F_\ell$ and $G_\ell$ are respectively regular and irregular solutions for neutron waves, and $\rho v_\ell$ is the penetration factor. Quantities $a_\ell$ and $b_\ell$ are related to the resonance terms by the formulae

$$a_\ell \rho^2 v_\ell^2 = \sum_\lambda \frac{\frac{1}{2}\Gamma_{\lambda s\ell}\Gamma_\lambda}{(E_\lambda - E)^2 + \frac{1}{4}\Gamma_\lambda^2} \quad , \tag{A-4}$$

and

$$b_\ell \rho v_\ell = \sum_\lambda \frac{\Gamma_{\lambda s\ell}(E_\lambda - E)}{(E_\lambda - E)^2 + \frac{1}{4}\Gamma_\lambda^2} \quad . \tag{A-5}$$

Although the quantities $a_\ell$ and $b_\ell$ are still dependent on the energy, these can be supposed as constants in the energy region far from the resonances.

The right hand side of Eq.(A-3) is given as follows for the s-wave:

$$1 - (1 - a_0\rho^2)\cos 2\rho - b_0\rho \sin 2\rho$$

$$= \sum_{n=0}^{\infty} \left\{ \frac{(-)^n}{(2n+2)!} 2^{2(n+1)} + \frac{(-)^n}{(2n)!} 2^{2n} a_0 - \frac{(-)^n}{(2n+1)!} 2^{2n+1} b_0 \right\} \times \rho^{2(n+1)} . \tag{A-6}$$

For low energy ($\rho << 1$), main term is one for n=0, which is proportional to $\rho^2$, that is $k^2R^2$. This means that the total cross section is proportional to $2\pi R^2$ at zero energy. It is found in Eq.(A-6) that the total cross section can be expanded in even powers of $\rho$ for the s-wave in the low energy region. This is the main reason why the total cross section of carbon can be expressed by the low order polynomial of the energy.

For the p-wave, Eq.(A-3) is written as

$$1 - \cos 2\rho + \{ a_1\rho^2 v_1^2 + 2v_1(1-a_1\rho^2 v_1^2) + 2b_1 v_1^2 \} \cos 2\rho - \frac{1}{1+\rho^2}\{2(1-a_1\rho^2 v_1^2) + b_1 v_1(1-\rho^2)\}\rho \sin 2\rho. \quad \text{(A-7)}$$

and for the d-wave,

$$1 - \cos 2\rho + \left\{ a_2\rho^2 v_2^2 + (1-a_2\rho^2 v_2^2) \frac{18\rho^2}{9+3\rho^2+\rho^4} + b_2 v_2 \frac{18\rho^2-6\rho^4}{9+3\rho^2+\rho^4} \right\} \cos 2\rho - \frac{1}{9+3\rho^2+\rho^4} \{ (1-a_2\rho^2 v_2^2)(18-6\rho^2) + b_2 v_2 (9-15\rho^2+\rho^4) \} \rho \sin 2\rho. \quad \text{(A-8)}$$

These two formulae are more complicated than Eq.(A-6). These, however, can also be expanded in even powers of $\rho$. Besides, it is easy to see that Eqs.(A-7) and (A-8) do not include the $\rho^2$-terms, that is, their first terms are higher order than that of Eq.(A-6).

Appendix B.

As mentioned in section 4, a fourth order polynomial is adopted as an empirical expression of the carbon total cross section,

$$\sigma_{nT}(E) = a_0 + a_1 E + a_2 E^2 + a_3 E^3 + a_4 E^4 , \quad \text{(B-1)}$$

where $a_i (i=0 \sim 4)$ are unknown parameters to be looked for. Least squares method gives the most probable values of the unknown parameters $a_i$, if the distributions of the experimental data of the cross section satisfy the conditions of the statistics and obey the rule of the normal distributions.

According to the principle of the least squares method, a value of Eq.(B-1) at a certain energy $E=E_r$ is the most probable value of the cross section $\sigma_{nT}(E_r)$, provided $a_i$ are the most probable values of the parameters. The parameters $a_i$ are obtained by solving the following normal equation, i.e.

$$\begin{bmatrix} A_{0,0} & A_{0,1} & A_{0,2} & A_{0,3} & A_{0,4} \\ \vdots & & & & \vdots \\ A_{4,0} & \cdots & \cdots & \cdots & A_{4,4} \end{bmatrix} \begin{bmatrix} a_0 \\ \vdots \\ a_4 \end{bmatrix} = \begin{bmatrix} C_0 \\ \vdots \\ C_4 \end{bmatrix} . \qquad \text{(B-2)}$$

Matrix (A) is a symmetric one, and the elements of the matrix, $(A_{ij})$, and constant vector, $(C_i)$, are given as follows,

$$\begin{aligned} A_{ij} &= \sum_{r=1}^{N} W_r E_r^{i+j} \\ C_i &= \sum_{r=1}^{N} W_r \sigma_{exp}(E_r) E_r^{i} \quad , \end{aligned} \qquad \text{(B-3)}$$

where $W_r$ is a weight of the experimental data $\sigma_{exp}(E_r)$. Solutions of Eq.(B-2) are the most probable values of the parameters $a_i$. Variance of the most probable value from the true value of the cross section is also given by the propagation of variances for $a_i$ from their true values. The variances and weights of the parameters $a_i$ are obtained by using a variance matrix (B) which is defined as an inverse matrix of the matrix (A). The weights $P_i$ of the parameters $a_i$ are defined by the relations

$$P_i = \frac{1}{B_{i,i}} \quad , \qquad \text{(B-4)}$$

and the variances $\delta_i^2$ are

$$\delta_i^2 = B_{i,i} \times \varepsilon^2 \quad , \qquad \text{(B-5)}$$

where $\varepsilon^2$ is the variance of the experimental data. The variance $\varepsilon^2$ is defined as follows, when population variance of the experimental data is unknown

$$\varepsilon^2 = \frac{1}{N-5} \sum_{r=1}^{N} W_r(\sigma_{exp}(E_r)-\sigma_{nT}(E_r))^2. \qquad \text{(B-6)}$$

The variance $\delta^2$ of $\sigma_{nT}(E)$ is given by using the variance matrix (B) and the variance $\varepsilon^2$

$$\delta^2 = [1,E,E^2,E^3,E^4] \begin{bmatrix} B_{0,0} & B_{0,1} & B_{0,2} & B_{0,4} \\ \vdots & & & \vdots \\ B_{4,0} & \cdots & \cdots & B_{4,4} \end{bmatrix} \begin{bmatrix} 1 \\ E \\ E^2 \\ E^3 \\ E^4 \end{bmatrix} \times \varepsilon^2. \qquad \text{(B-7)}$$

Confidence intervals of true values for the parameters $a_i$ and for the cross section $\sigma_{nT}(E)$ are obtained under a given confidence level, for example of 95 %. In this case, they are

$$[a_i - 1.96\delta_i, a_i + 1.96\delta_i], \qquad \text{(B-8)}$$

and

$$[\sigma_{nT}(E) - 1.96\delta(E), \sigma_{nT}(E) + 1.96\delta(E)], \qquad \text{(B-9)}$$

respectively.

Table I. Measurements on Total Neutron Cross Section of Carbon up to 2 MeV

| Authors | Lab. | Year | Ref. | Energy range* (eV) | Number of data points** | Errors assigned by authors*** | Method | Sample | Remarks |
|---|---|---|---|---|---|---|---|---|---|
| Walton et al. | GA | 1960 | BAPS 5 288 | 0.003-10 | 1 | | LINAC 30-$BF_3$ TOF | | Note 1 and 2 |
| Houk & Wilson | HRV | 1967 | RMP 39 546 | 0.3-400 | 1 | 0.0045b | TOF | pyrolytic graphite | Note 1 and 3 |
| Rayburn & Wollan | ORL | 1965 | NP 61 381 | 1.44 | 2 | 0.03b<br>0.06b | reactor<br>indium foil | graphite, diamond dust | Note 1 and 4 |
| Egelstaff | HAR | 1952 | SCISRS | 4.26-590 | 49 | (13%) | TOF | | Note 5 and 6 |
| Simpson et al. | MTR | 1964 | NIM 30 293 | 5-1,000 | 55 | (13.6%) | reactor, chopper $BF_3$ TOF | 0.75" thick, 3" thick | Note 5 and 7 |
| Brugger et al. | MTR | 1956 | PR 104 1054 | 14-10,000 | 74 | 0.10b | reactor, chopper $BF_3$ TOF | $CCl_4$, C 0.1582 atoms/b reactor grade | Note 5 and 8 |
| Triftshäuser & Fehsenfeld | MUNCH | 1965 | EANDC(E) 57"U" 21 | 33.9<br>61.1 | 2 | 0.002b<br>0.0024b | reactor filter-difference method $BF_3$ | graphite, polystyrene | Note 1 and 9 |
| Uttley & Diment | HAR | 1968 | EANDC (UK) 94 AL | 74-1.56M | 87 | (0.3-1.1%)<br>0.5%: 1 keV | LINAC $^{10}B$+NaI(Tl) TOF | 0.0842 atoms/b<br>0.2997 atoms/b reactor grade | Note 1 and 10 |
| Hibdon | ANL | 1954 | SCISRS | 1.1k-160k | 109 | (6-15%) | | | Note 5 and 11 |

| Authors | Lab. | Year | Ref. | Energy range* (eV) | Number of data points** | Errors assigned by authors*** | Method | Sample | Remarks |
|---|---|---|---|---|---|---|---|---|---|
| Seth et al. | DKE | 1963 | NP 47 137 | 3k-660k | 684 | 2% net error 0.08b:3-500k 0.12b:500-660k | VdG, Li(p,n) $BF_3$ 20°&160°collimator | 0.228 atoms/b reactor grade with no moisture | Note 1 and 12 |
| Mooring et al. | ANL | 1966 | NP 82 16 | 10k-550k | 55 | 0.02-0.03b | VdG, Li(p,n) 2 systems of 34-$BF_3$ 255k, $\theta$ =135° 280k, $\theta$ =45° | 0.04263 atoms/b 0.06447 atoms/b 0.12780 atoms/b 0.31688 atoms/b 4.4 cm$\phi$ | Note 1 and 13 |
| Miller | WIS | 1950 | PR 78 806 | 20k-1360k 806 | 2 | 5% | | | Note 5 and 14 |
| Fields et al. | ANL | 1947 | PR 71 508 | 24k-830k | 6 | | photon neutron sources | $B_4C$ | Note 5 and 15 |
| Frisch | LAS | 1946 | PR 70 589 | 35k-490k | 4 | (3-4%) | VdG, Li(p,n) proton recoil prop. counter | 0.376 ± 0.001" thick 3/4"disk | |
| Kiehn et al. | MIT | 1953 | PR 91 66 | 50k-1080k | 55 | | VdG, Li(p,n) proton recoil counter | graphite, $CCl_4$ 2.5cm$\phi$ x 2.5cm | Note 5 and 17 |
| Allen & Ferguson | HAR | 1955 | PPS A68 1077 | 60k-550k | 5 | 1%: 120k 3%: others | VdG, Li(p,n) hydrogen filled prop. counter | 2"$\phi$ x 0.9" | Note 1 and 18 |
| Whalen et al. (1) | ANL | 1967 | Private com. | 100k-650k | 546 | 1-3% | VdG, Li(p,n) 24-$BF_3$ DCB | 1"$\phi$ disk transmission 0.6 ~ 0.75 | Note 1 and 19 |
| Cance et al. | BRC | 1970 | GF N° 187/W | 100k-1200k | 21 | 3% | VdG, Li(p,n) stilben, DCB | | Note 1 and 20 |

| Authors | Lab. | Year | Ref. | Energy range* (eV) | Number of data points ** | Errors assigned by authors*** | Method | Sample | Remarks |
|---|---|---|---|---|---|---|---|---|---|
| Wilenzick et al. | DKE | 1961 | PR 121 1150 | 180k-700k | 103 | 0.1b | VdG, Li(p,n)<br>2" x 2" plastic<br>TOF | 1-2" disks<br>0.253 atoms/b<br>0.339 atoms/b | Note 5 and 21 |
| Bretscher & Martin | CAV | 1950 | HPA 23 15 | 0.22M-2.0M (4.1M) | 7 (12) | 5% | VdG, C(d,n), D(d,n)<br>proton recoil prop. counter | 3.8 cmϕ,<br>graphite<br>1-10 cm thick | Note 5 and 22 |
| Bailey et al. | MIN | 1946 | PR 70 583 | 0.35M-2.0M (6.0M) | 7 (20) | (1.3-3.7%) | VdG, Li(p,n),C(d,n)<br>Ar filled ionization chamber with proton radiator | $C_6H_{12}$, C | Note 5 and 23 |
| Schwarz et al. | NBS | 1970 | BAPS 15 567 | 0.49M-2.0M (15M) | 2070 (3363) | 2% | LINAC<br>TOF | 0.47 atoms/b<br>1.68 atoms/b | Note 1 and 24 |
| Huddleston et al. | ANL | 1960 | PR 117 1055 | 0.5M-1.35M | 660 | 2.7% | VdG, Li(p,n)<br>ionization chamber<br>DCB | pile grade<br>1.5"ϕ x 0.9" | Note 1 and 25 |
| Freier et al. | MIN | 1950 | PR 78 508 | 0.6M-1.9M | 12 | 5% | VdG, Li(p,n)<br>Ar filled ionization chamber with thin layer of paraffin | $0.205 \times 10^{23}$ atoms/$cm^2$<br>1.5"ϕ disk | Note 5 and 26 |
| Smith & Whalen | ANL | 1969 | Private com. | 0.6M-1.4M | 5 | (0.8-1.5%) | VdG<br>Mono. $E_n$, DCB | | Note 1 and 27 |
| Cabe et al. | SAC | 1963 | EANDC (E) 49L 69 | 0.64M-1.0M | 76 | 3% | VdG, T(p,n)<br>Stilben, DCB | | Note 1 and 28 |
| Whalen et al. (2) | ANL | 1969 | Private com. | 0.65M-1.55M | 451 | | VdG<br>Mono. $E_n$, DCB | | Note 1 and 29 |

| Authors | Lab. | Year | R Ref. | Energy range* (eV) | Number of data points** | Errors assigned by authors*** | Method | Sample | Remarks |
|---|---|---|---|---|---|---|---|---|---|
| Cierjacks et al. | KFK | 1968 | Washington Conf. (II) 743 | 0.67M-2.0M (30M) | 2118 (4318) | 3% | cyclotron liquids scinti., TOF | | Note 1 and 30 |
| Yergin et al., | RPI | 1966 | Washington Conf. (I) 690 | 0.75M-2.0M (50M) | 427 (931) | 3-5% | LINAC 20"$\phi$ x 5" liquid scinti., TOF | | Note 1 and 31 |
| Lampi et al. | MIN | 1950 | PR 80 853 | 0.8M-2.0M (5.0M) | 10 (12) | 2% | VdG, Li(p,n) Ar filled ironization chamber with paraffin radiator 5 cm$\phi$ x 9 cm | $C_6H_{12}$ graphite disk | Note 32 |
| Bockelman et al. | WIS | 1951 | PR 84 69 | 1.25M-2.0M (3.3M) | 38 (122) | 2-3% | VdG, T(p,n) proton recoil I.C. 2.5 cm$\phi$ x 9.5 cm | graphite 4.45 cm | Note 33 |
| Storrs & Frisch | MIT | 1954 | PR 95 1252 | 1.315M | 1 | 0.020b (0.9%) | VdG, Li(p,n) proton recoil prop. counter, DCB | $CH_2$, 3/8-5/8" thick C, 1" thick | Note 1 and 34 |

* Numbers in parentheses indicate the maximum neutron energy reported in the original references.

** Numbers in parentheses indicate the total number of experimental data points obtained by original authors.

*** Numbers in parentheses indicate the percent errors calculated by the present authors using the absolute experimental errors (in barns) reported in the original references.

## Notes for Table I

Note 1. The numerical data are accepted as the input data of Data Set No. 2 for making least-squares fit in the present evaluation for the total neutron cross section of carbon. The weight factor $a_j$ assigned by the present authors is equal to 1 in Eq.(3-3).

Note 2. Walton et al.: Over a broad energy region centered near 0.025 eV, the cross-section value of 4.77 ± 0.05 barns is obtained; which is about 15 % higher than Egelstaff's data, JNE 5, 203 (1957). The cross-section value is cited from AERE-PR/NP 13 (1968).[44)]

Note 3. Houk & Wilson: Check of the n-p incoherent cross section. Pyrolytic graphite is free of over molecular binding and coherent scattering effects above 0.3 eV. The cross-section value is 4.7534 barns.

Note 4. Rayburn & Wollan: No description for sample purity and the error assignment. This report covers completely the contents of Phys. Rev. 87, 174 (1952). The cross-section values are 4.66 and 4.74 barns for the samples of graphite and diamond dust, respectively.

Note 5. The numerical data are not accepted as the input data of Data Set No. 2 for making least-squares fit in the present evaluation, in accordance with the criterion mentioned in the text.

Note 6. Egelstaff: Only the numerical data from SCISRS were available, without any description of the experimental condition.

Note 7. Simpson et al.: The cross-section measurements were made rather for experimental verification of the background determination than to obtain accurate cross-section values, and no error assignment was given for the cross-section value in the paper. From this reason a large weight may not be assessed to these data, although the good agreement of the cross-section data for two different sample thicknesses shows quality of the data.

Note 8. Brugger et al.: The aim of the experiment is to measure the total cross section of C1. The cross-section curve for carbon shows a flat behaviour within ± 0.5 barns, and the cross-section value is given to be 4.69 ± 0.10 barns as an averaged value.

Note 9. Triftshäuser & Fehsenfeld: The purpose is to get a better information about the n-p interaction. The samples of polystyrene and graphite are used. The filter materials used are $^{10}B$, Rh, Cd, Mn and Co. The cross-section values are 4.743 and 4.7264 barns at the energies of 33.9 and 61.1 eV, respectively.

Note 10. Uttley & Diment: Keeping their minds on the usefulness of carbon total cross section as standard one, the measurements were performed. A polynomial formula is given below 1.5 MeV, i.e., $\sigma_{nT} = 4.744 - 3.707E + 2.389E^2 - 1.114E^3 + 0.242E^4$, E is energy in MeV and $\sigma_{nT}$ in barns. A thin $^{10}B$ plus was viewed by four NaI(Tl) to form a detector for neutrons over 70 eV $\leq$ En $\leq$ 100 keV at 120 m station. A much thicker plug of $^{10}B$ metal powder was located at 300 m as the similar detector, which covered the energy region 10 keV to 10 MeV.

Note 11. Hibdon: The error assignments are typically given to only 4 data points out of 109. They are 15 %, 11 %, 8 % and 6 % at the energies of 2.6 keV 4.6 keV, 9.5 keV and 17.5 keV, respectively. No informations on the experimental condition were obtained from SCISRS.

Note 12. Seth et al.: A polynomial formula, $\sigma_{nT} = 4.95 - 4.24E + 2.23E^2$, E in MeV, is given. The rms error of the least-squares polynomial is 0.14b. The resolution widths is $\simeq$ 300 eV at 10 keV and rises to $\sim$ 1 keV at 300 keV with 160° arrangement of the incident beam. With 20° arrangement, it is $\sim$ 800 eV at 150 keV and falls to $\sim$ 500 eV at 650 keV. The net error includes an estimated maximum error of 1 % in the sample thickness. In the energy region 400 keV to 660 keV, the cross-section data join smoothly with the data

of Freier et al., Miller, and Bockelman et al. Almost all data (581 data points out of 681) were in the energy range from 500 keV to 660 keV, since the measurements were performed in order to find out the levels at 610 keV.

Note 13. Mooring et al.: In order to correct sample impurity in the measurements of $\sigma_{nT}$ for $^{10}B$, $^{11}B$ and $\sigma_a$ for $^{11}B$, $\sigma_{nT}$ of carbon and oxygen were measured. Carbon is used as a pure scatterer. The results agree with Seth's data above 200 keV and consistently lower than Seth's data below 200 keV. Difference increases with neutron energy decrease. The data also agree with the curve of Huddleston formula (4.71 b at thermal energy). The energy spread of incident neutron is 10 keV.

Note 14. Miller: Search for energy level in $^{13}C$. The cross sections monotonically decrease from 4.8 b at 20 keV to 2.4 b at 1.36 MeV. Standard statistical error is less than 5 %. The results agree with the data of Lampi et al. and Wattenberg[25] within 3 %.

Note 15. Fields et al.: No error assignment for carbon cross sections.

Note 16. Frisch: The correction was applied for single scattering into the chamber because of the finite sizes of the scatterer and detector.

Note 17. Kiehn et al.: The purpose of the experiment was to obtain the $\sigma_{nT}$ of Cl. Corrections were made for the carbon content in the $CCl_4$ sample by measuring the $\sigma_{nT}$ of carbon. The number of data points is counted from Fig. 1 of original paper. No information about the error assignment by authors. For $0.15 \leq E_n \leq 0.75$ MeV, $\Delta E_n \leq$ 2-4 keV step; for $0.75 \leq E_n \leq 1.1$ MeV, $\Delta E_n \simeq 25$ keV. The step of 30 keV is taken in the energy range 0.4 - 1 MeV. In-scattering correction is less than 1 %.

Note 18. Allen & Ferguson: The purpose is n-p cross section measurement. The original paper is a research note, and the measurements are made at 60, 75, 90, 120 and 550 keV.

Note 19. Whalen et al.(1); A computer controlled experiment. The relative energy resolution is about 2.5 keV and the intervals are 1 keV below 650 keV. The statistical error varies from 1 to 3 %.

Note 20. Cance et al.: The energy spread is 30 keV to 40 keV, and the step is 50 keV. The results agree with the data of Seth et al., Wilenzick et al. and Freier et al. The n-$\gamma$ discrimination is used. The error of 3 % consists of statistical and geometrical ones.

Note 21. Wilenzick et al.: Detailed study of resonance structure by using time-of-flight (TOF) method. Standard deviations is about 0.1b and maximum deviation is 0.2b. The energy spread is about 5 keV. According to one of the authors, K. K. Seth, we were informed that there was uncertainty of about 10 % in the determination of backgrounds in time spectra. He recommended the use of another data produced by the direct-current-beam (DCB) method by Seth et al.

Note 22. Bretscher & Martin: In order to determine the hydrogen cross section by using paraffine scatterers, authors had to measure the carbon cross section. Final error was estimated to be not more than 5 %.

Note 23. Bailey et al.: The neutron energy spread is rather larger than usual, for example 100 keV at 1 MeV. Frisch's data is more accurate in the energy range below 0.5 MeV. There was fluctuation in neutron source intensity.

Note 24. Schwarz et al.: The overall energy resolution is about 0.1 ns/m. The overall accuracy including statistical and absolute error is about 2 %. The energy calibration agrees with Wisconsin Group.

Note 25. Huddleston et al.: The experiment aims to observe resonances corresponding to states in the $^{11}B(^{3}He,p)^{13}C$ reaction. Better energy resolution less than 5 keV and the greater sensitivity provided by the

self-indication technique are employed. The step of 1 keV is chosen in the vicinity of 610 keV and 1250 keV, and the step of 2 keV elsewhere. A polynomial expression is given in the energy region from 500 keV to 1350 keV; i.e., $\sigma_{nT} = 4.710 - 3.415E + 1.649E^2 - 0.2606E^4$, where E is in MeV and $\sigma_{nT}$ in barns. The rms error in this region is 0.075 barns or an average of 2.7 %.

Note 26. Freier et al.: Statistical error is 5 % and the neutron energy spread 30 keV. The counter efficiency is energy sensitive and is proportional to $E_n^2$ above 500 keV. The number of data points is counted from Fig. 1, in which four data points with vertical bars are obtained from the n-p scattering measurement by Lampi et al., PR 76, 186A (1949). In that case, the statistical error was reduced to about 1 % and energy spread about 15 keV.

Note 27. Smith & Whalen: Symmetrical collimated geometry. The energy spread is 5 keV. Statistical errors of 0.8 - 1.5 % are assigned for the cross-section values at the checking energy points of 0.606, 0.805, 1.204, and 1.403 MeV. The T-O-F technique is combined with the D-C-B measurement. It is aimed to resolve the discrepancy between LINAC and VdG data.

Note 28. Cabe et al.: The results agree with the data of Wilenzick et al. in the energy region from 600 to 700 keV, but disagree with the data of Huddleston et al. in the order of 100 - 150 mb. The neutron energy spread is about 8 keV and the step of the measurement about 5 keV.

Note 29. Whalen et al.(2): The computer controlled experiment, same as Note 19. The energy range measured is extended from 650 keV up to 1.5 MeV. The step and accuracy of the measurement is 2 keV and about 1 %, respectively.

Note 30. Cierjacks et al.: High resolution total cross-section measurements, where overall resolution is less than 0.03 ns/m. Statistical accuracy is typically 1 %. The numerical data used for the present evaluation are those obtained recently from the CCDN (August 1970), which include the correction

for the systematic errors caused by dead-time effects in time-of-flight experiments.

Note 31. Yergin et al.; The statistical uncertainties are 3 to 5 %. Overall time resolution is about 0.25 ns/m with an 100-m flight path.

Note 32. Lampi et al.: The correction for finite geometry of the experiment was made by measuring the cross section of the scatterer area and extrapolating to zero area. The statistical uncertainty in $\sigma_{nT}$ was calculated from the extrapolation formula and the reproducibility of the cross section for each scatterer during the run. The probable errors assigned to the cross section include the uncertainty in the background count and the uncertainty in the correction for the low energy group of neutrons. The cross sections are reliable to about 2 %. The data are accepted as the input data with the weight factor $a_j$=0.5, taking into account that the measurement were made almost 20 years ago.

Note 33. Bockelman et al.: The errors of 2-3 % are statistical one. A correction of 1.5 % for scattering into the detector was applied to all the measured scattering cross section, assuming the scattering were isotopic. Measured backgrounds amounted about 2 % of the intensity observed in the absence of the shadow cone. The neutron energy spread resulting from the thickness of the Zr-T target was about 20 keV. The data are accepted as the input data with the weight factor $a_j$ = 0.5, taking into account that the measurements were almost 20 years ago.

Note 34. Storrs & Frisch: Precise measurement of H(n,n). Aiming for a determination of the singlet n-p range to the order of $0.1 \times 10^{-13}$ cm, they needed to know the energy to 10 keV and the cross section to 0.2 percent. Corrections for obtaining the polyethylene and carbon cross section are reported in detail in Table I of the original paper. The averaged carbon cross section obtained is 2.192 ± 0.010 b, where the error is statistical only. Energy point of 1.315 ± 0.003 MeV corresponds to the strong resonance of oxygen cross section.

Table II. Contents of Data Set No. 1 and No. 2

| Data Set No. 1 | Data Set No. 2 | |
|---|---|---|
| | Group (A) | Group (B) |
| Egelstaff[18] | | Walton et al.[15] |
| Simpson et al.[19] | | Houk and Wilson[16] |
| Brugger et al.[20] | | Rayburn and Wollan[17] |
| Uttley and Diment[8] | Uttley and Diment[8] | Triftshaüser and Fehsenfeld[21] |
| Hibdon[22] | | Allen and Ferguson[28] |
| Seth et al.[7] | Seth et al.[7] | Storrs and Frisch[43] |
| Fields et al.[25] | | |
| Whalen et al.(1)[29] | Whalen et al.(1)[29] | Mooring et al.[23] |
| Bretscher and Martin[32] | | Cance et al.[30] |
| Bailey et al.[33] | | Schwarz et al.[34] |
| Cabe et al.[37] | Cabe et al.[37] | Huddleston et al.[6] |
| Yergin et al.[40] | Yergin et al.[40] | Smith and Whalen[36] |
| Lampi et al.[41] | Lampi et al.[41] | Whalen et al.(2)[38] |
| Bockelman et al.[42] | Bockelman et al.[42] | Cierjacks et al.[39] |
| 14 data sets<br>2,184 data points | 20 data sets<br>7,758 data points | |

Notes: Data Sets No. 2 contains two groups of data sets (A) and (B). According to the weight consideration for quality of individual data sets, seven data sets in Data Set No. 1 were not adopted in Data Set No. 2. The rest among Data Set No. 1 is listed as group (A).

Newly added data sets to Data Set No. 1 are listed as group (B). The upper six data sets in group (B) have relatively small number of data points (see Table 1).

Table III. Recommended cross-section values of $\sigma_{nT}(E)$ calculated from Eq.(4-11), which is derived from fitting the experimental data (Data Set No. 2) by the least-squares method with the weight of $a_j \frac{1}{\sqrt{N_j}\ (\Delta\sigma_{ij})^2}$.

| E(MeV) | $\sigma_{nT}$(barns) | E(MeV) | $\sigma_{nT}$(barns) |
|---|---|---|---|
| 0.000 | 4.699 | 1.000 | 2.586 |
| 0.050 | 4.549 | 1.050 | 2.522 |
| 0.100 | 4.404 | 1.100 | 2.461 |
| 0.150 | 4.274 | 1.150 | 2.438 |
| 0.200 | 4.129 | 1.200 | 2.347 |
| 0.250 | 3.999 | 1.250 | 2.294 |
| 0.300 | 3.787 | 1.300 | 2.243 |
| 0.350 | 3.754 | 1.350 | 2.195 |
| 0.400 | 3.639 | 1.400 | 2.148 |
| 0.450 | 3.528 | 1.450 | 2.104 |
| 0.500 | 3.422 | 1.500 | 2.061 |
| 0.550 | 3.321 | 1.550 | 2.019 |
| 0.600 | 3.223 | 1.600 | 1.979 |
| 0.650 | 3.130 | 1.650 | 1.939 |
| 0.700 | 3.041 | 1.700 | 1.901 |
| 0.750 | 2.956 | 1.750 | 1.863 |
| 0.800 | 2.875 | 1.800 | 1.826 |
| 0.850 | 2.798 | 1.850 | 1.821 |
| 0.900 | 2.724 | 1.900 | 1.752 |
| 0.950 | 2.653 | 1.950 | 1.715 |
| 1.000 | 2.586 | 2.000 | 1.677 |

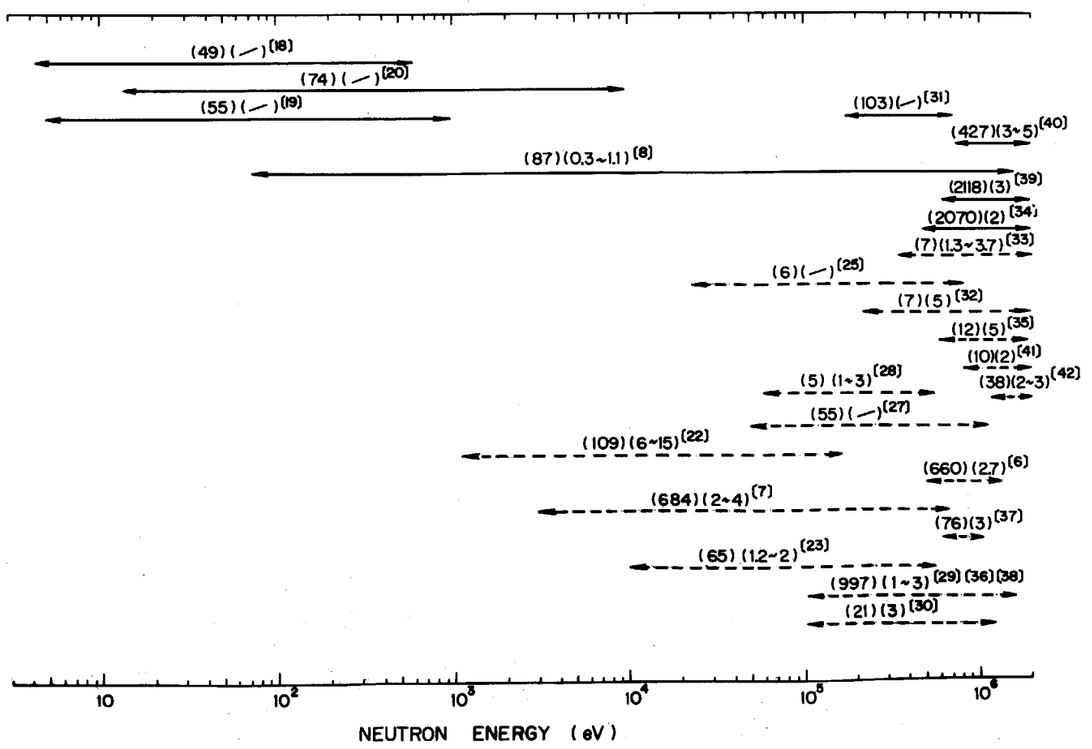


Fig. 1. Energy range of original data. The lines of ⟷ and ←- - -→ show the energy regions, in which the data are measured by the time-of-flight (TOF) and direct-beam-current (DCB) method, respectively. The numbers in the 1st, 2nd and 3rd parentheses represent the number of data points, percent errors and reference numbers, respectively.

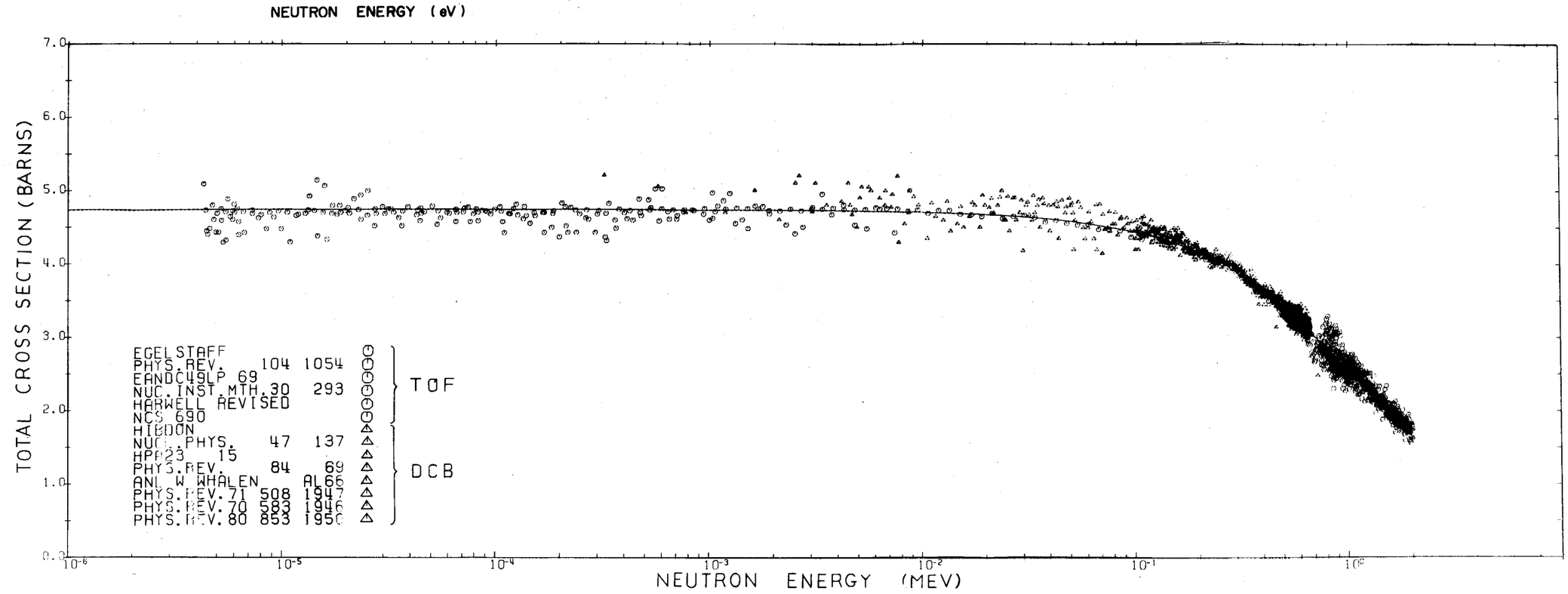


Fig. 2. The total neutron cross-section data of carbon (Data Set No. 1) from 1 eV up to 2 MeV. The solid curve represents Eq.(4-5), which is an empirical formula deduced by the least-squares method with the weight of $W_{ij}=1/(\Delta\sigma_i)^2$.

This is a blank page.

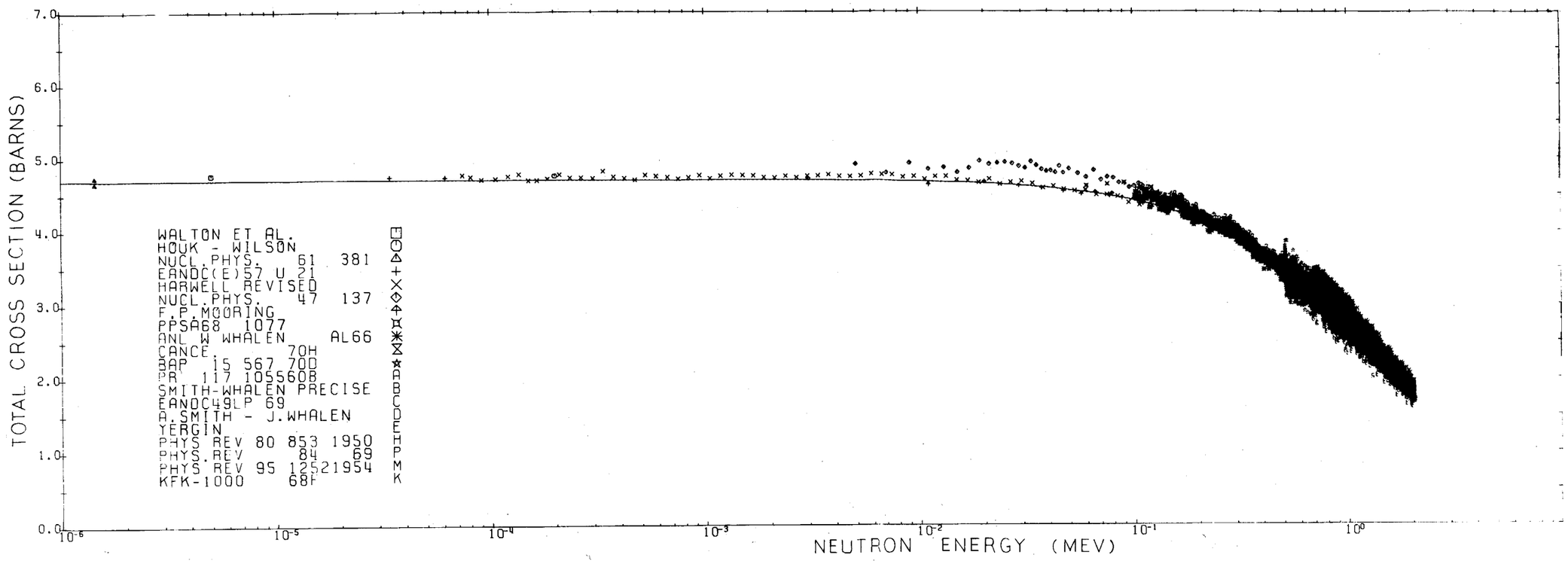


Fig. 3. The total neutron cross-section data of carbon (Data Set No. 2) from 1 eV up to 2 MeV. The solid curve represents Eq. (4-11), which is a recommended empirical formula deduced by the least-squares method with the weight of $W_{ij}=a_j/\sqrt{N_j}(\Delta\sigma_{ij})^2$.

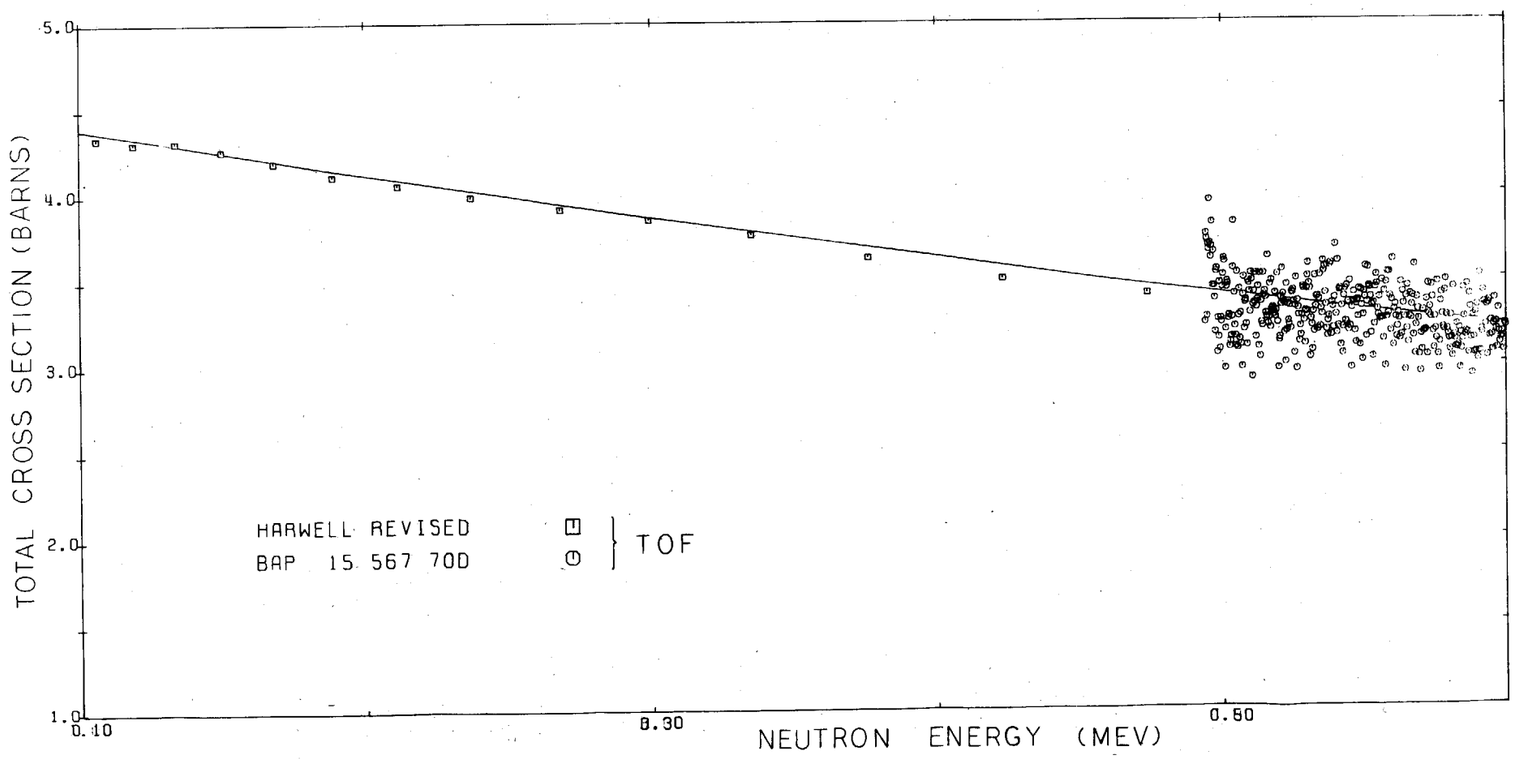


Fig. 4. The total neutron cross-section data of carbon (Data Set No. 2) from 100 keV to 600 keV, which were measured by TOF method. The data are the same as those of the energy range in Fig. 3, but the energy scale is enlarged. The solid curve represents Eq. (4-11).

This is a blank page.

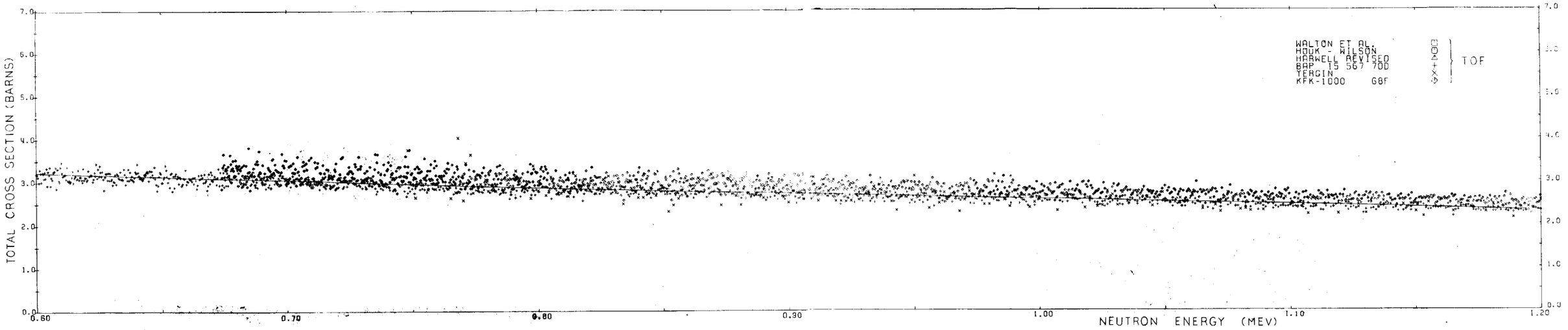


Fig. 5. The total neutron cross-section data of carbon (Data Set No. 2) from 600 keV to 1.2 MeV, which were measured by TOF method. (See figure caption of Fig. 4).

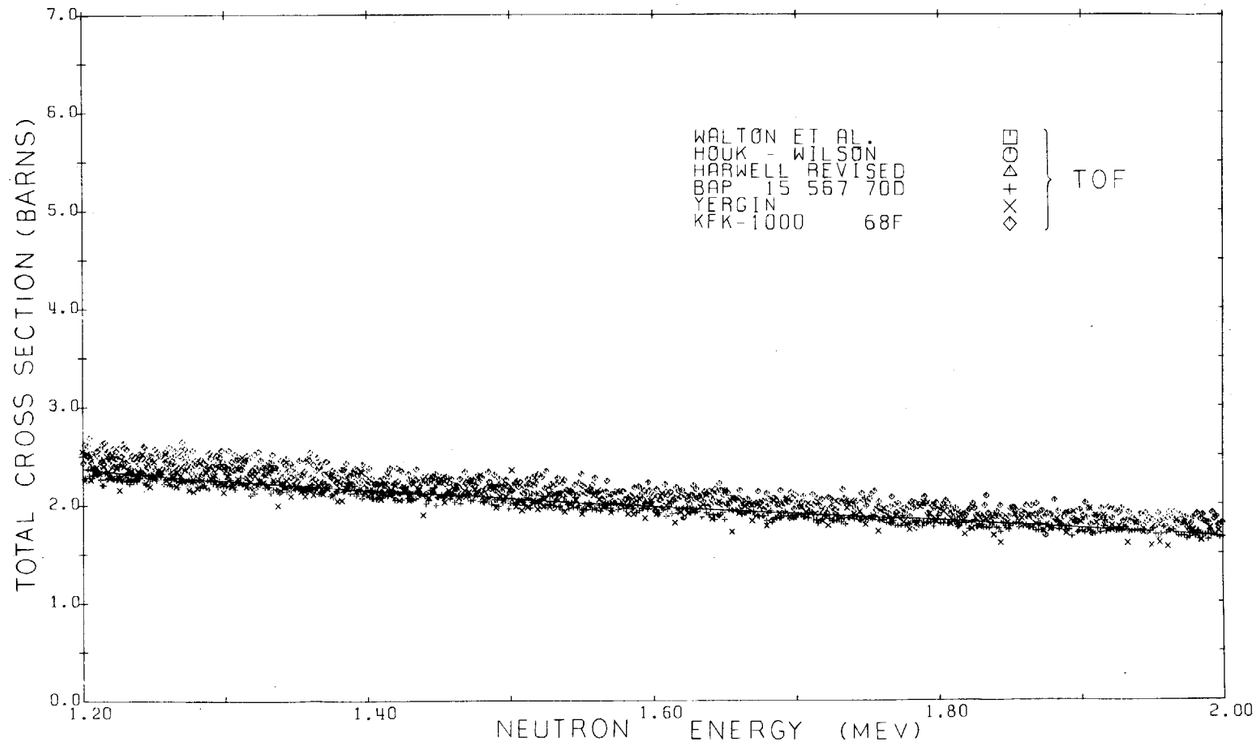


Fig. 6. The total neutron cross-section data of carbon (Data Set No. 2) from 1.2 MeV to 2.0 MeV, which were measured by TOF method. (See figure caption of Fig. 4).

This is a blank page.

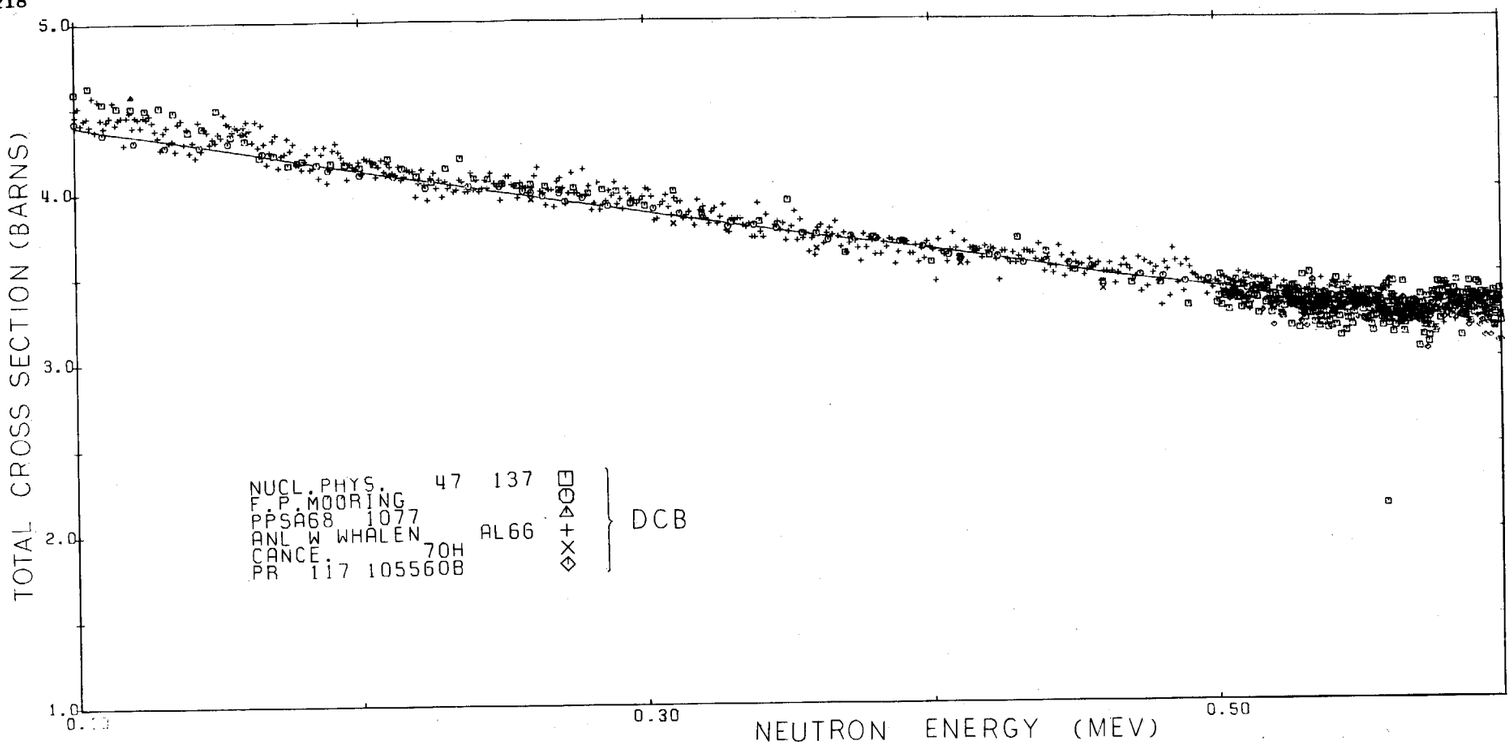


Fig. 7 The total neutron cross-section data of carbon (Data Set No. 2) from 100 keV to 600 keV, which were measured by DCB method. The data are the same as those of the energy range in Fig. 3, but the energy scale is enlarged. The solid curve represents Eq.(4-11), which is recommended empirical formula deduced by the least-squares method with the weight of $W_{ij}=a_j/\sqrt{N_j}(\Delta\sigma_{ij})^2$.

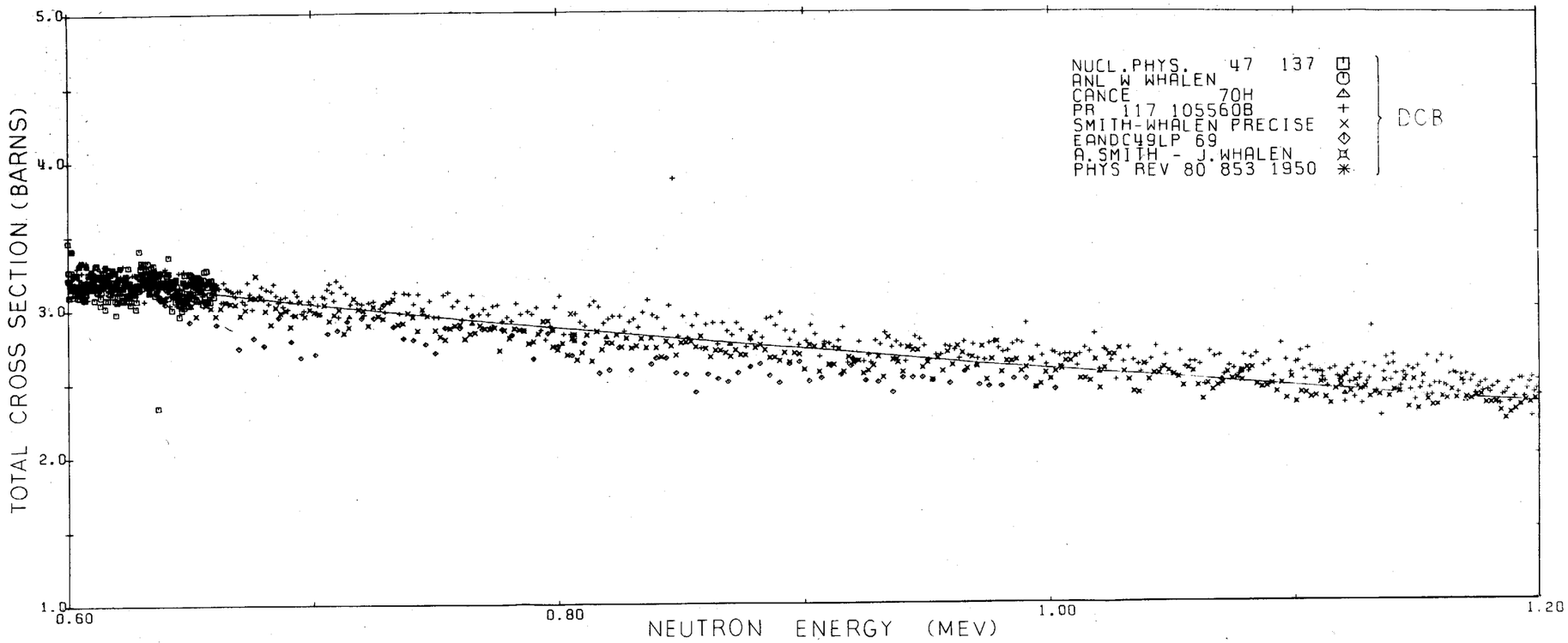


Fig. 8. The total neutron cross-section data of carbon (Data Set No. 2) from 600 keV to 1.2 MeV, which were measured by DCB method. (See figure caption of Fig. 7).

This is a blank page.

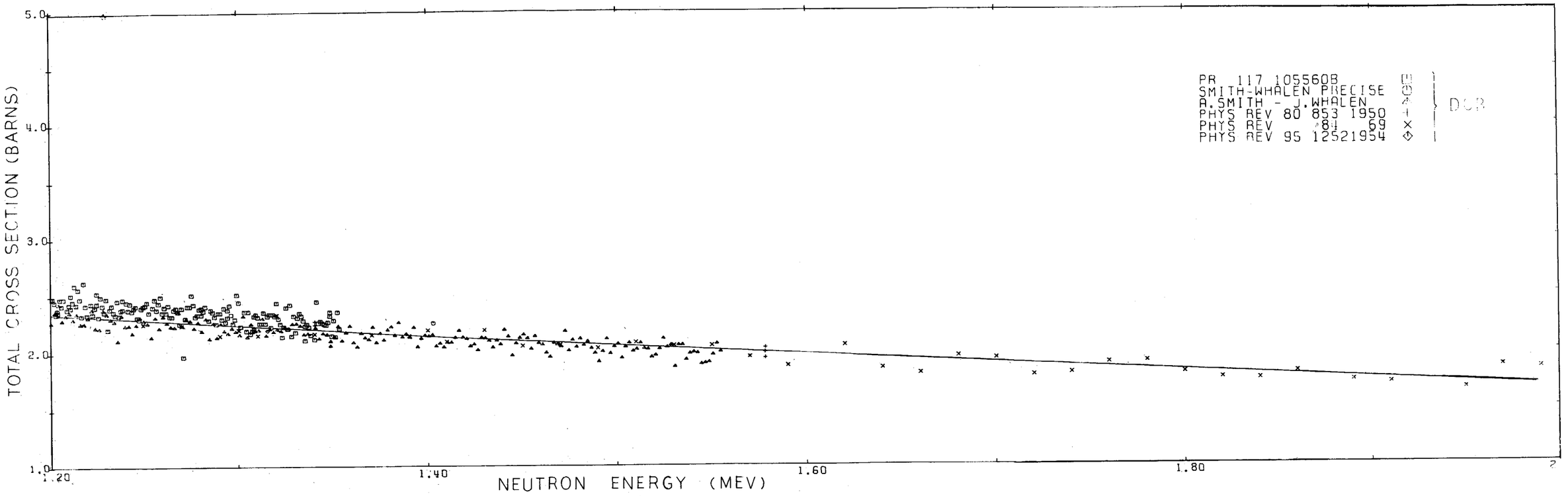


Fig. 9. The total neutron cross-section data of carbon (Data Set No. 2) from 1.2 MeV to 2.0 MeV, which were measured by DCB method. (See figure caption of Fig. 7).

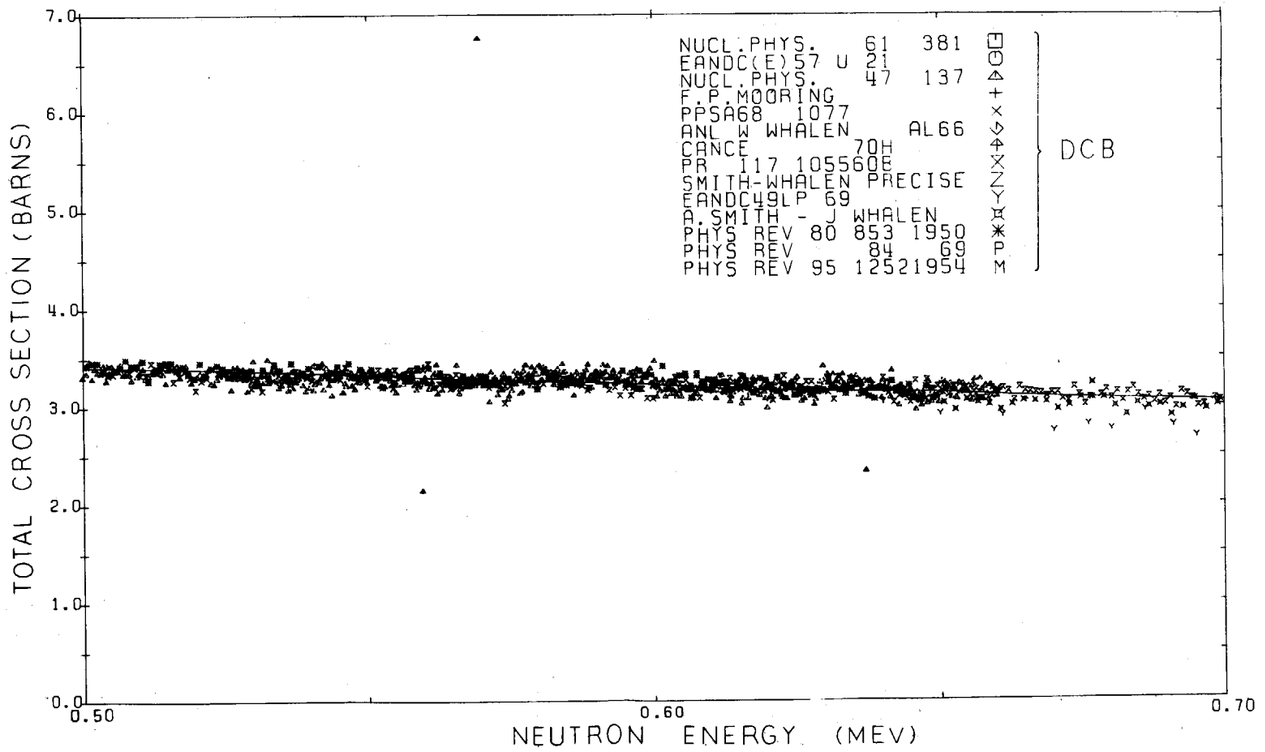


Fig. 10. The total neutron cross-section data of carbon (Data Set No. 2), from 500 keV - 700 keV, measured by DCB method. The data are the same as those in the energy range of Fig. 3. The energy scale is further enlarged at the most dense parts of the data in Figs. 7 and 8. The solid curve represent Eq.(4-11), which is a recommended empirical formula deduced by the least-squares method with the weight of $W_{ij}=a_j/\sqrt{N_j}(\Delta\sigma_{ij})^2$.

This is a blank page.

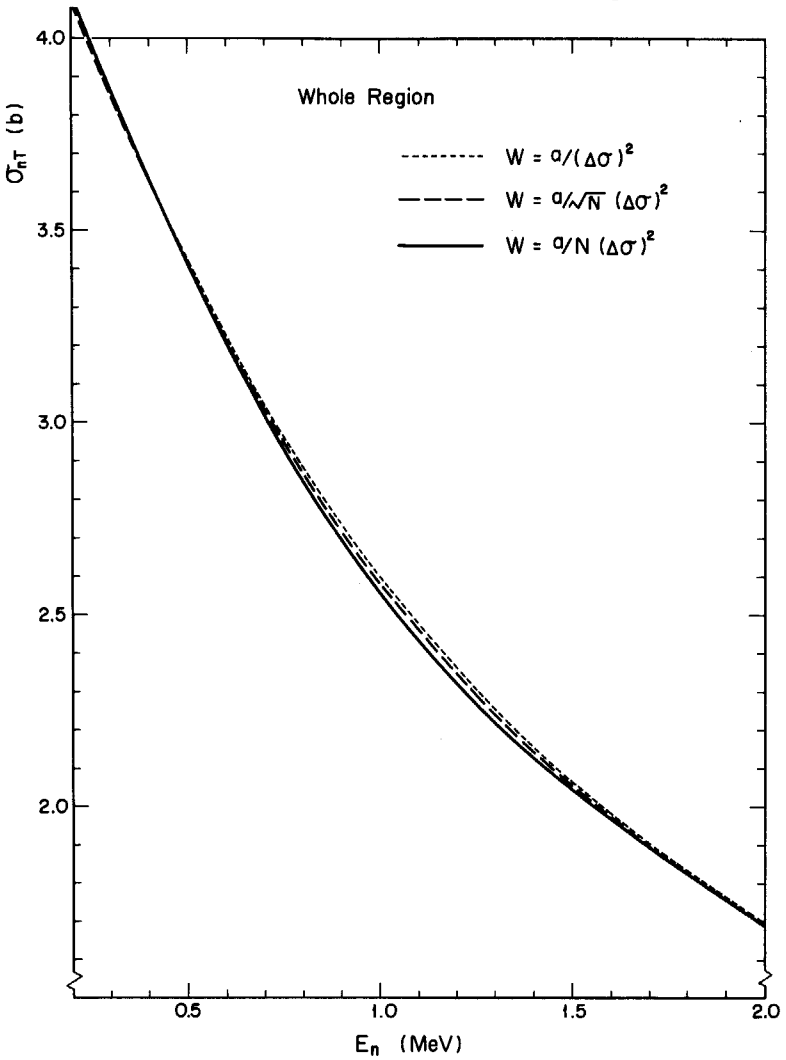


Fig. 11. Cross section curves obtained with Data Set No. 2, and with the weights $W_{ij}=a_j(\Delta\sigma_{ij})^2$, $W_{ij}=a_j/\sqrt{N_j}(\Delta\sigma_{ij})^2$ and $W_{ij}=a_j/N(\Delta\sigma_{ij})^2$. These curves correspond to Eqs. (4-10), (4-11) and (4-12).

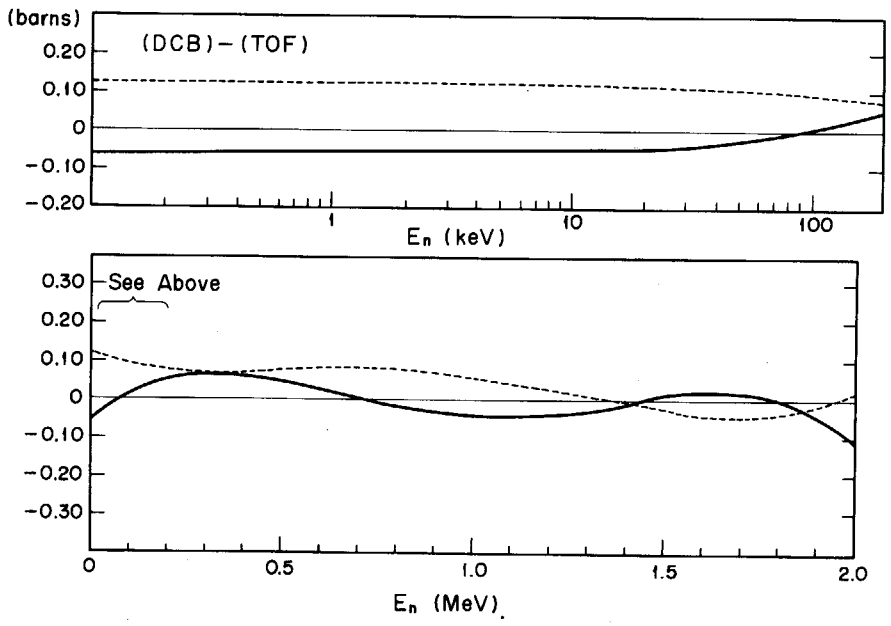


Fig. 12. Differences between the results of the least-squares fitting applied to the DCB and TOF data. The dotted line shows the difference for the $a_j/(\Delta\sigma_{ij})^2$ treatment (Eq.(4-8)-Eq.(4-9), Data Set No. 1) and the solid line the difference for the $a_j/\sqrt{N_j}(\Delta\sigma_{ij})^2$ treatment (Eq.(4-13)-Eq.(4-14), Data Set No. 2).

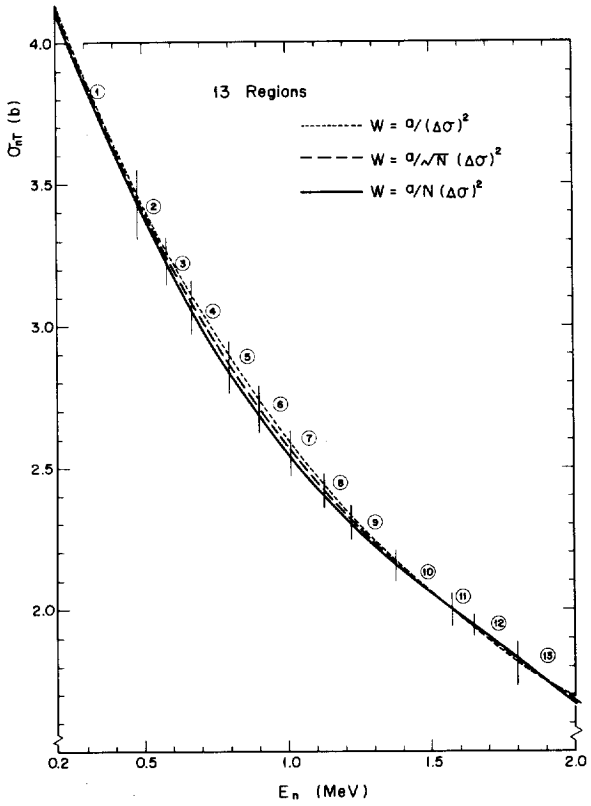


Fig.13. Cross-section curves in the case that the energy region is divided into 13 sub-regions, except for the dotted curve (Data Set No. 2), which is plotted for comparison. These curves are obtained from the following formulae:

Dotted curve: Eq.(4-10),

Dashed curve: $\sigma_{nT}(E) = 4.699 - 3.098E + 1.099E^2 - 0.094E^3 - 0.029E^4$, (F-1)

Solid curve: $\sigma_{nT}(E) = 4.705 - 3.145E + 1.035E^2 + 0.031E^3 - 0.070E^4$, (F-2)

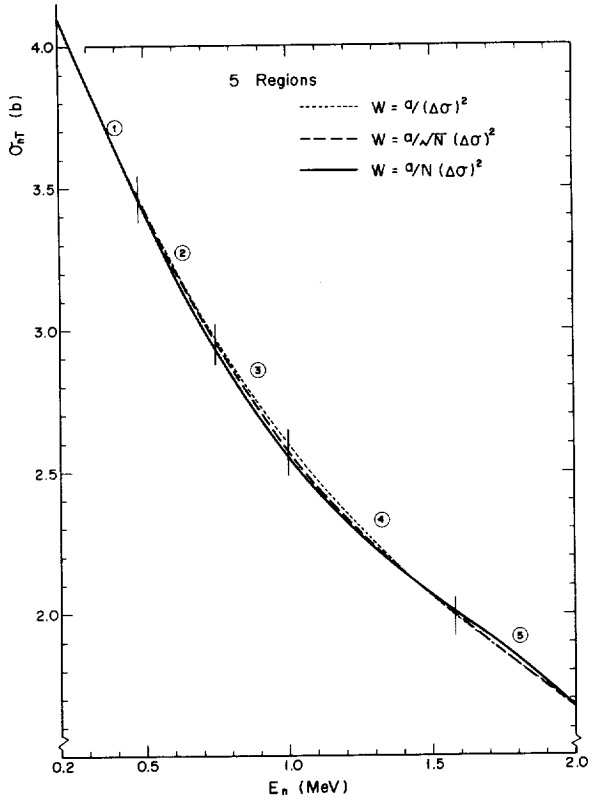


Fig. 14. Cross-section curves in the case that the energy region is divided into 5 sub-regions, except for the dotted curve (Data Set No. 2), which is plotted for comparison. These curves are obtained from the following formulae:

Dotted curve: Eq.(4-10),

Dashed curve: $\sigma_{nT}(E) = 4.699 - 3.050E + 0.968E^2 + 0.013E^3 - 0.056E^4$, (F-3)

Solid curve: $\sigma_{nT}(E) = 4.705 - 3.031E + 0.744E^2 + 0.262E^3 - 0.128E^4$. (F-4)

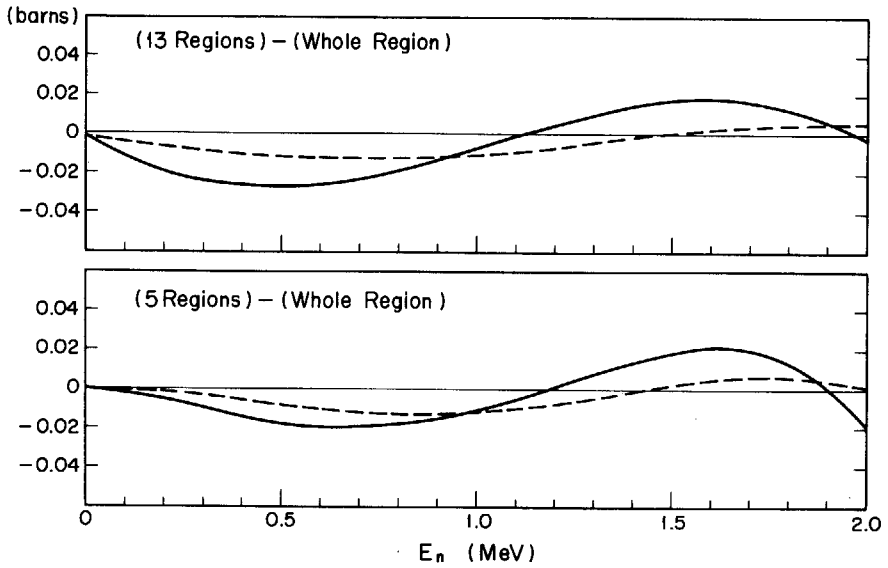


Fig. 15. Differences between the curves with and without the division of the energy region in the cases of weights $a_{je}/\sqrt{N_{je}}(\Delta\sigma_{ij})^2$ and $a_{je}/N_{je}(\Delta\sigma_{ij})^2$.
(dashed line of upper figure) = Eq.(F-1) - Eq.(4-11),
(solid line of upper figure) = Eq.(F-2) - Eq.(4-12),
(dashed line of lower figure) = Eq.(F-3) - Eq.(4-11),
(solid line of lower figure) = Eq.(F-4) - Eq.(4-12).

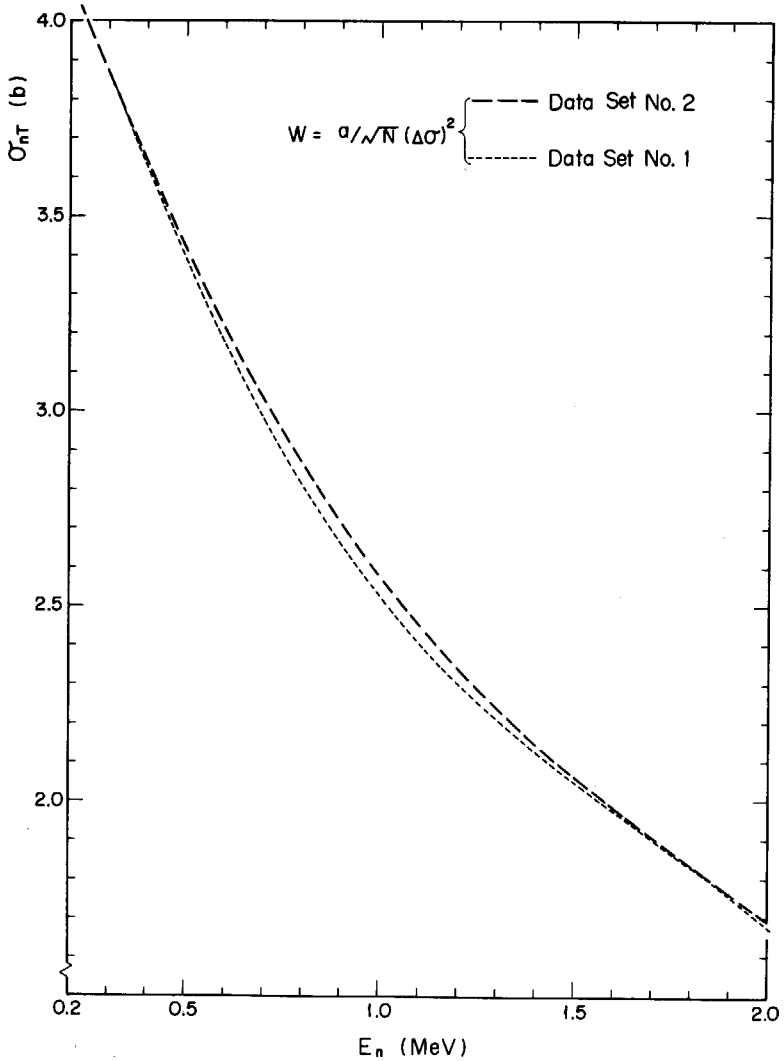


Fig. 16. Comparison between the cross-section curve Eq. (4-11) (dashed line) obtained with Data Set No. 2 and the curve Eq.(5-1) (dotted line) obtained with Data Set No. 1.

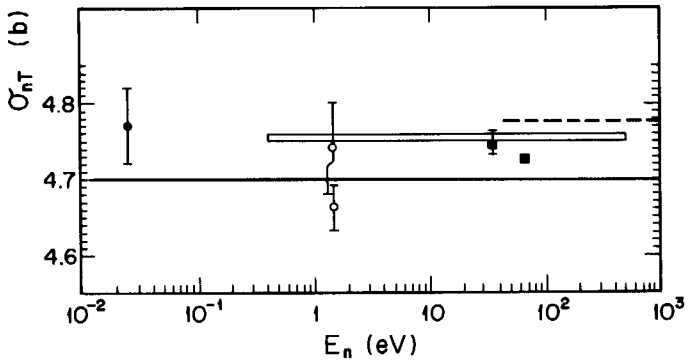


Fig. 17. Cross-section values below 1 keV. The solid and dashed lines are the present values of Eq.(4-11) and Harwell values[8], respectively. The open circles are the data of Rayburn and Wollan[17], the closed circle the data of Walton et al.,[15)44)] and the squares the data of Triftshäuser and Fehsenfeld.[21] The horizontally long rectangle represents the uncertainty of the energy range and cross-section value of Houk and Wilson.[16]

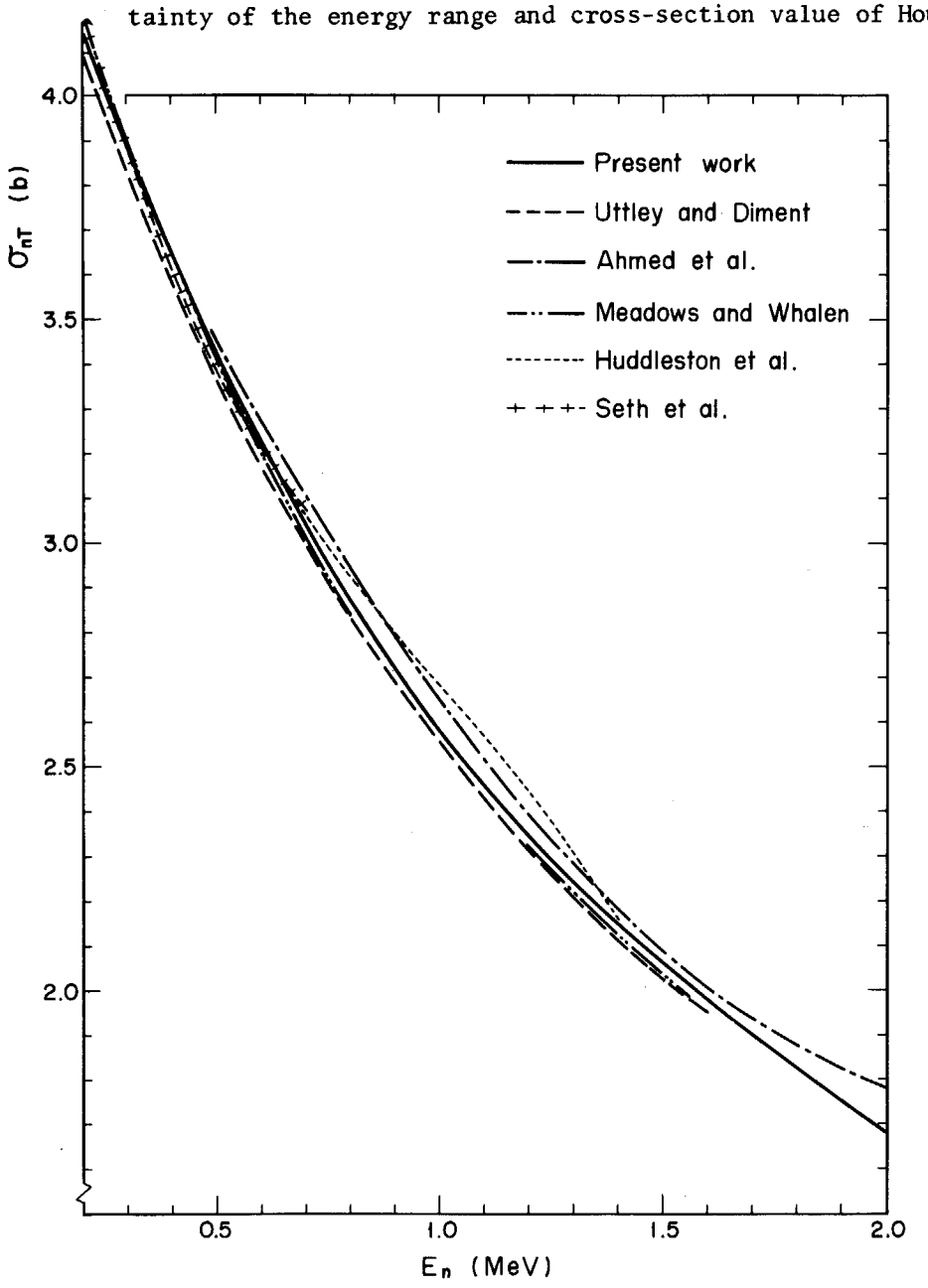


Fig. 18. Comparison of the present cross-section curve of Eq.(4-11) ($W_{ij}=a_j/\sqrt{N_j}(\Delta\sigma_{ij})^2$ with the cross-section curves of other authors.

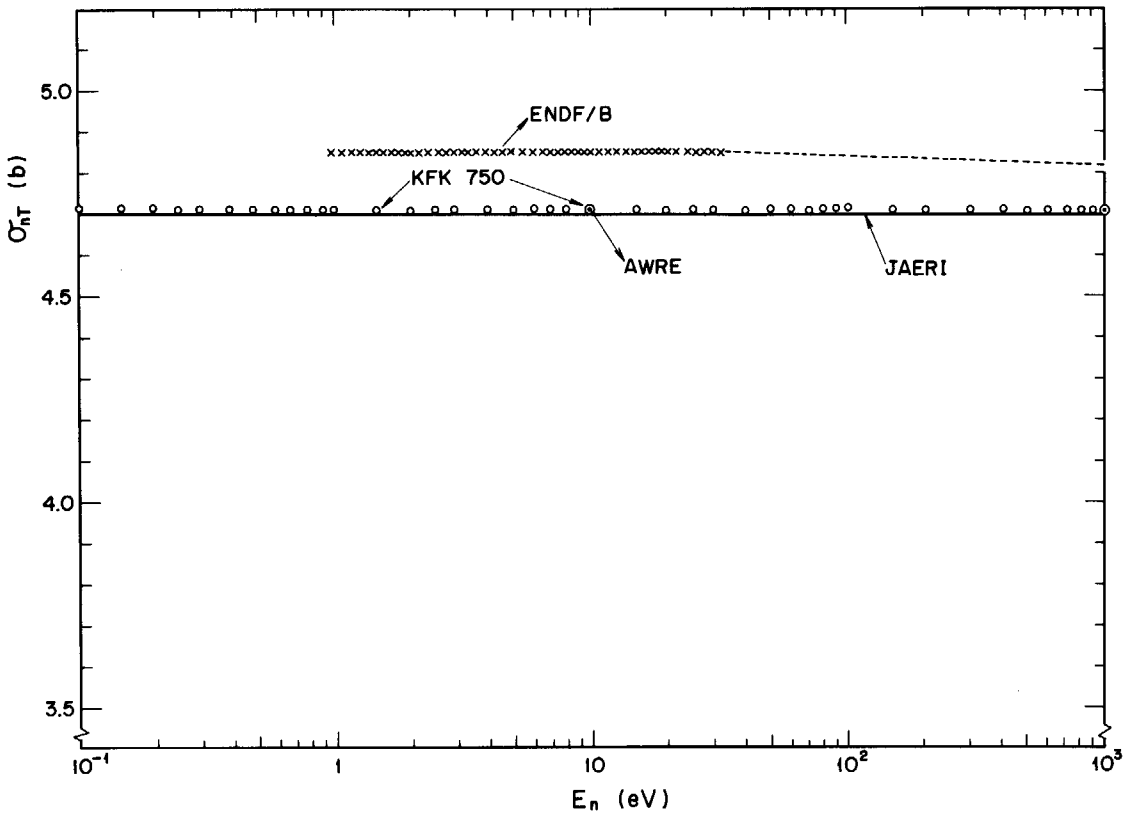


Fig. 19. Comparison of the present cross-section curve (JAERI) of Eq.(4-11) ($W_{ij}=a_j/\sqrt{N_j}(\Delta\sigma_{ij})^2$) with those of other data files in the eV region.

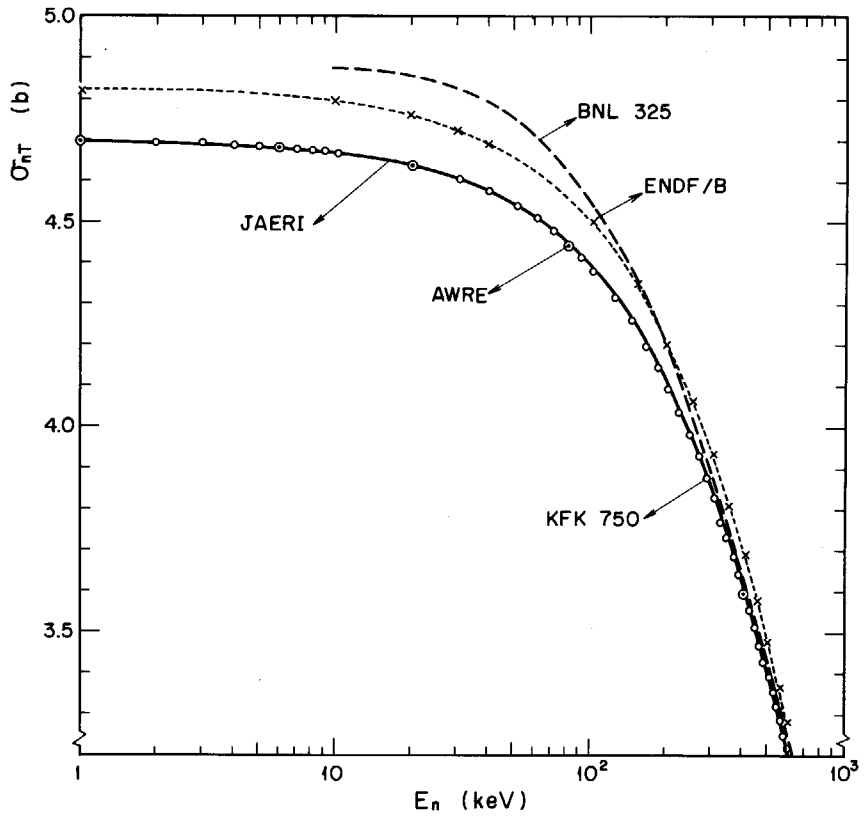


Fig. 20. Comparison of the present cross-section curve (JAERI) of Eq.(4-11) ($W_{ij}=a_j/\sqrt{N_j}(\Delta\sigma_{ij})^2$) with those of other data files in the keV region.

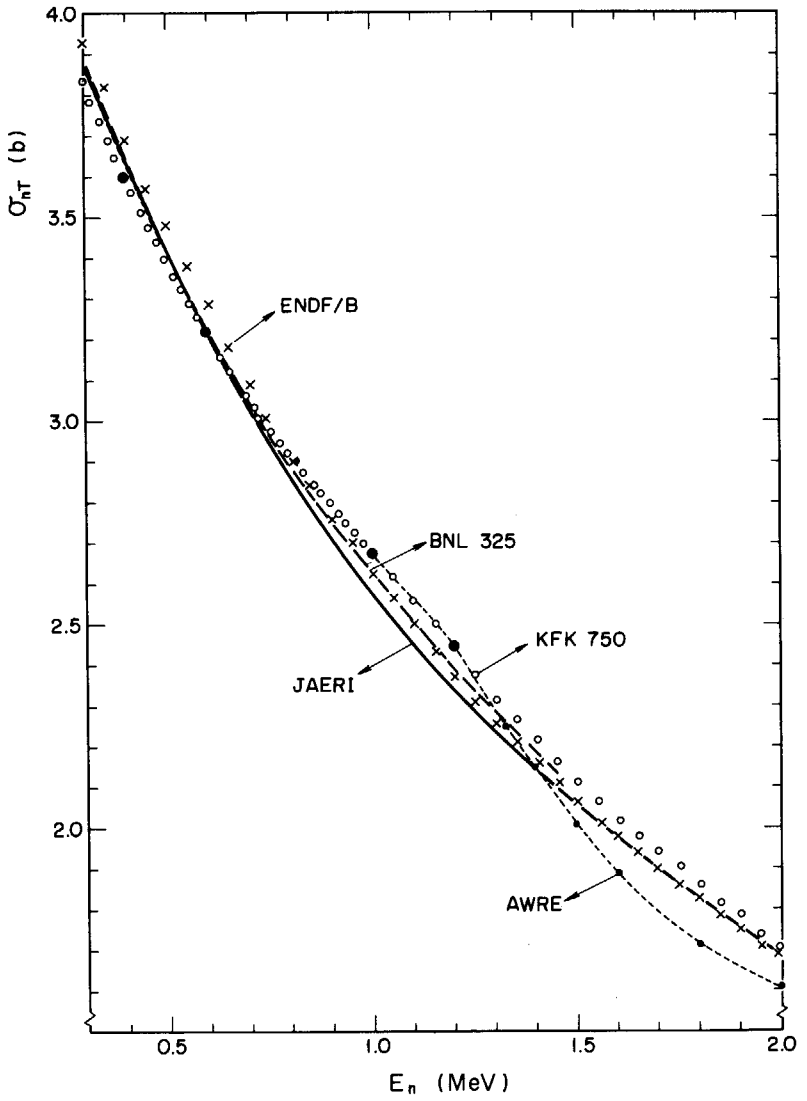


Fig. 21. Comparison of the present cross-section curve (JAERI) of Eq.(4-11) ($W_{ij}=a_j/\sqrt{N_j}(\Delta\sigma_{ij})^2$) with those of other data files in the MeV region.